LABORATORI NAZIONALI DI FRASCATI
SIS – Pubblicazioni

LNF-95/016 (P)
5 Aprile 1995

Multi-bunch Energy Spread induced by Beam Loading in a Standing Wave Structure

M. Ferrario #, A. Mosnier *, L. Serafini @,F. Tazzioli # , J.-M. Tessier*

*CEA/DAPNIA/SEA, CE-Saclay, 91191 Gif-sur-Yvette, France
#INFN, Lab. Naz. di Frascati, C.P.13,00044 Frascati (Roma),Italy
@INFN, Sez. di Milano, Via Celoria 16, 20133 Milano, Italy

Abstract

The interaction of a relativistic beam with the modes of the TM_{010} pass-band of a multicell cavity does not cause any problem: although all the modes are excited by the RF generator, resulting in different cell excitations during the cavity filling and the beam pulse, the net accelerating field exhibits negligible fluctuations from bunch to bunch. However, when the beam is not fully relativistic, this is no more true. The phase slippage occurring in the first cells, between the non relativistic beam and the lower pass-band modes, produces an effective enhancement of the shunt impedances, which is usually negligible for a relativistic beam in a well tuned cavity. Moreover, the voltage jumps (amplitude and phase) occurring at each bunch passage, as well as the beam detuning caused by the off-crest bunches, vary from cell to cell. These effects enhance dramatically the fluctuation of the accelerating voltage, with a dominant beating provided by the pass-band mode nearest to the pi-mode. The induced beam energy spread has been estimated by the help of two distinct codes, developed at Frascati and Saclay, with results in good agreement. While an interaction integral is computed at each bunch passage, the cavity refilling is calculated by solving coupled differential equations of the "modes" of the pass-band, driven by a generator linked to one end-cell. It is shown also that the intermode coupling arises from the external Q of the drive end-cell, and not from the wall losses. For illustration, we applied the method to the beam-loading problem in the SC capture cavity of the low charge injector of TESLA Test Facility installed at DESY.

PACS: 29.27.Bd

Submitted to Particle Accelerators

1. INTRODUCTION

In addition to single bunch effects, induced in particular by space charge forces, multi-bunch effects due mainly to propagation of the RF field wave will affect the quality of a non relativistic beam accelerated by standing wave structures. The study of these beam loading effects, which could limit the performances of injectors involving SW cavities, led to the development of numerical codes : HOMDYN [1], which includes space charge effects and transverse motion and MULTICELL [2], which involves the longitudinal motion.

After a cavity filling time, the cavity is periodically refilled by RF power during the bunch to bunch interval. We are then first interested in the evolution of the field amplitude along the structure, driven by a generator, coupled to an end-cell. Although the generator frequency is set close to the accelerating pi-mode, all the "modes" of the TM_{010} pass-band will be excited. The transient behavior of driven standing-wave structures has been extensively studied for many years. In Ref. [3], for example, the multi-mode analysis permitted to explain the distortion of RF field responses to a pulse of pi-mode RF drive, by using Laplace transforms. More recently, in the aim to study the beam loading effect in the superconducting cavity TESLA for a relativistic and on-crest beam, the multi-mode problem was solved by using systems of first order differential equations [4] or Laplace transforms [5].

In this paper, we use however another approach, by directly solving the differential equations relative to each usual mode of the pass-band [6], provided that an intermode coupling term is taken into account. It can be shown in fact (see Appendices for further details), with the help of the theory of coupled resonators, that the usual "modes" of the pass-band, found in the steady-state regime and computed by cavity codes like Urmel, are coupled through the external Q of the first cell, and not through the intrinsic wall losses of the cells, due to the orthogonality relation of the eigenvectors. The excitations Z_m of these "normal modes" of index m are then found by solving the following system of coupled differential equations (equation B-3 of appendix B)

$$\ddot{Z}_m + \frac{\omega_o}{Q_o}\dot{Z}_m + T_{1m}\frac{\omega_o}{Q_{ex}}\sum_k T_{1k}\dot{Z}_k + \omega_m^2 Z_m = \frac{T_{1m}}{N\varepsilon}\frac{d}{dt}\int_S (\vec{n}\times H_n(\vec{r},t))E_{an}(\vec{r})\,dS - \frac{1}{\varepsilon}\frac{d}{dt}\int_{V_{cav}} J(\vec{r},t)\,E_a^m(\vec{r})\,dV \qquad (1)$$

The first driving terms represents the generator current, while the second integral along the whole cavity represents the beam interaction with the mode m and will be computed at each bunch passage.

The coefficient T_{nm} is the normalized excitation of mode m at the center of cell n.

The evolution of the fields for each mode of the pass-band during the cavity filling and during the bunch to bunch interval is found by numerically integrating the system (1) with the generator current as driving term. Since we are particularly interested in the evolution of amplitude and phase envelopes of the RF fields, which are slowly varying functions, this second order system can be easily transformed to a first order differential equations system. At each bunch passage, the longitudinal motion of the particles and the perturbation due to beam-loading on the field envelopes are obtained by numerical integration.

2. THE RELATIVISTIC CASE

The propagation of the RF pulse from the generator location through a multicell cavity (the 9-cell TESLA cavity) was simulated by using the differential equations reported in the Appendices. The field envelope at the center of the first and last cells during the cavity filling are shown on figure 1.

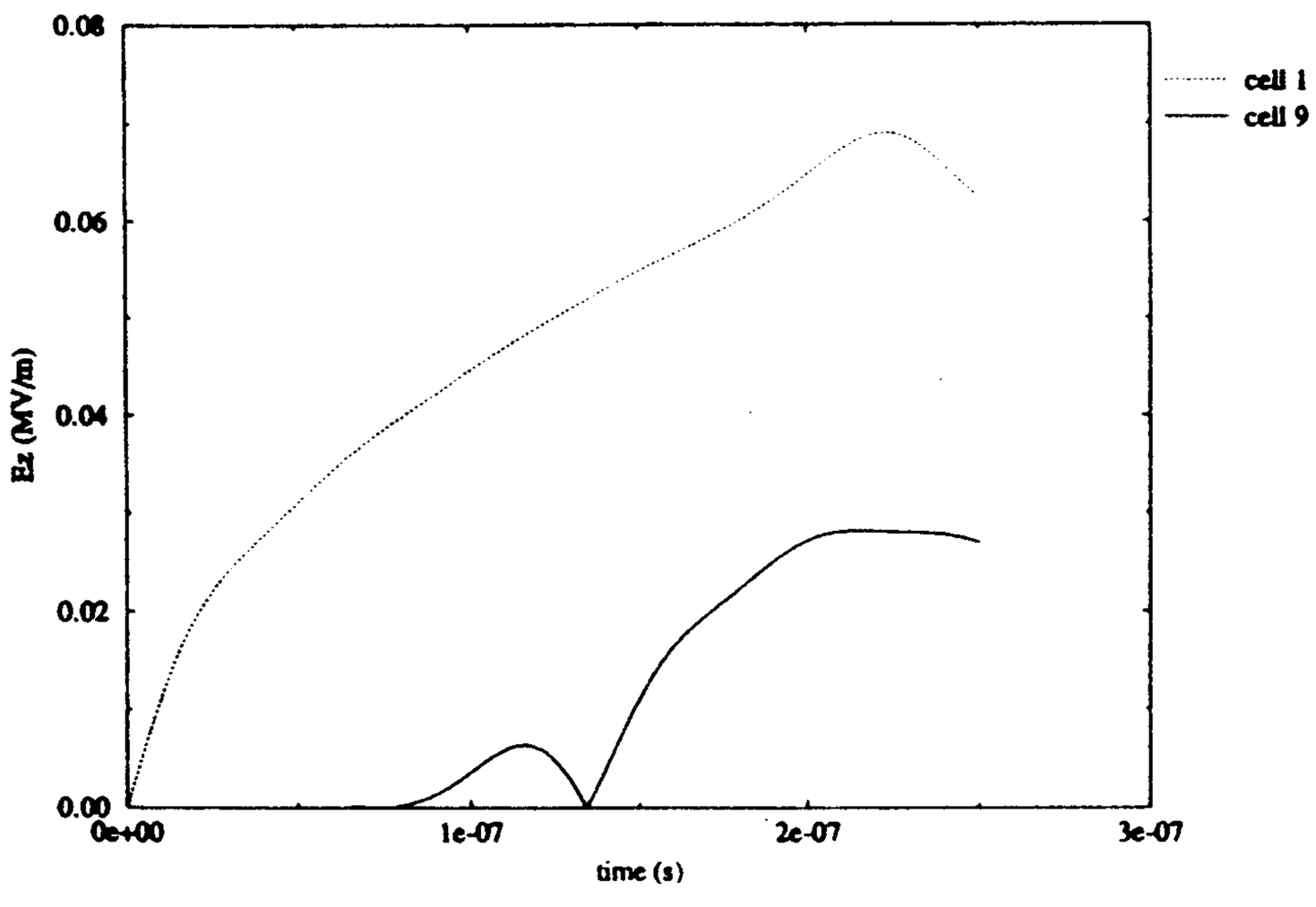

Figure 1 : field envelope at center of cells during the cavity filling

This transient behavior is similar to the one found in Ref [4]. With an expected gradient of 25 MV/m, the figure 2 shows the evolution of the E_z field at the center of the first and last cells, but during the beginning of the relativistic TESLA bunch train (bunch charge of 8 nC and bunch spacing of 1 μs) . The first bunch is injected after the pi-mode filling time $t_b = \tau_\pi \, Ln\, 2$. Figure 3 shows the accelerating fields, provided by all the individual cells and after averaging over all cells. It is worthwhile noting that the energy gain provided by the first and last cells is slightly smaller, because of the fringing field of the endcells, and that all bunches gain on average about the same energy amount. For a

well tuned cavity and with a relativistic beam, the average of the accelerating fields for all modes vanishes to zero, except of course for the pi-mode. However, since the pi-mode is coupled to the other excited modes through the Qex, some fluctuation remains. The figure 4, plot of the total accelerating voltage during the entire TESLA beam pulse, points out the residual oscillations, mainly caused by the nearest mode of the pass-band, decaying according to the time constants of the modes. The induced bunch-to-bunch energy spread is nevertheless very small, 3 10^{-6} at the beginning to 0.5 10^{-6} at the end.

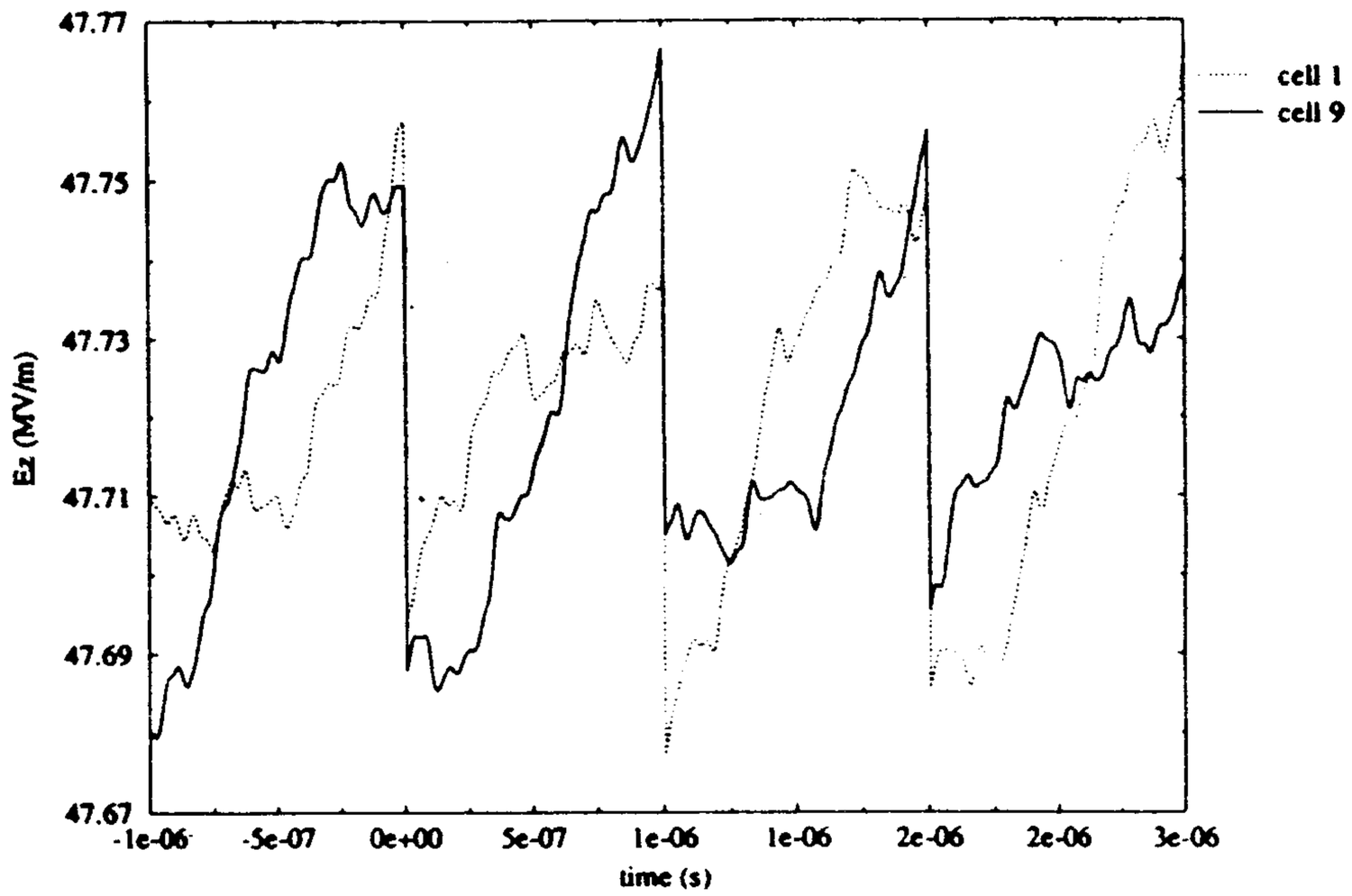

Figure 2 : E_z field at center of cells with a relativistic bunch train

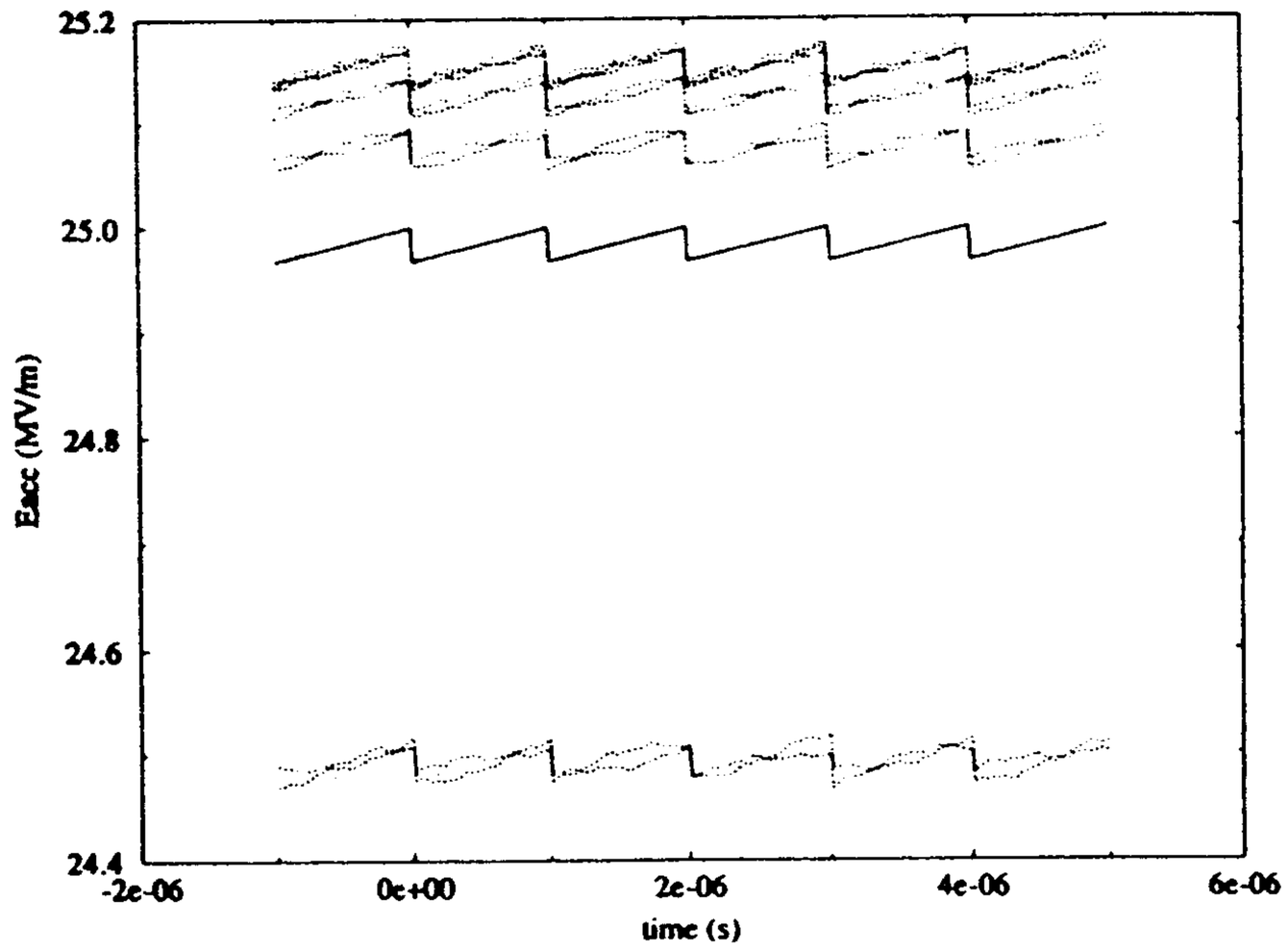

Figure 3 : cell accelerating fields and average with a relativistic bunch train

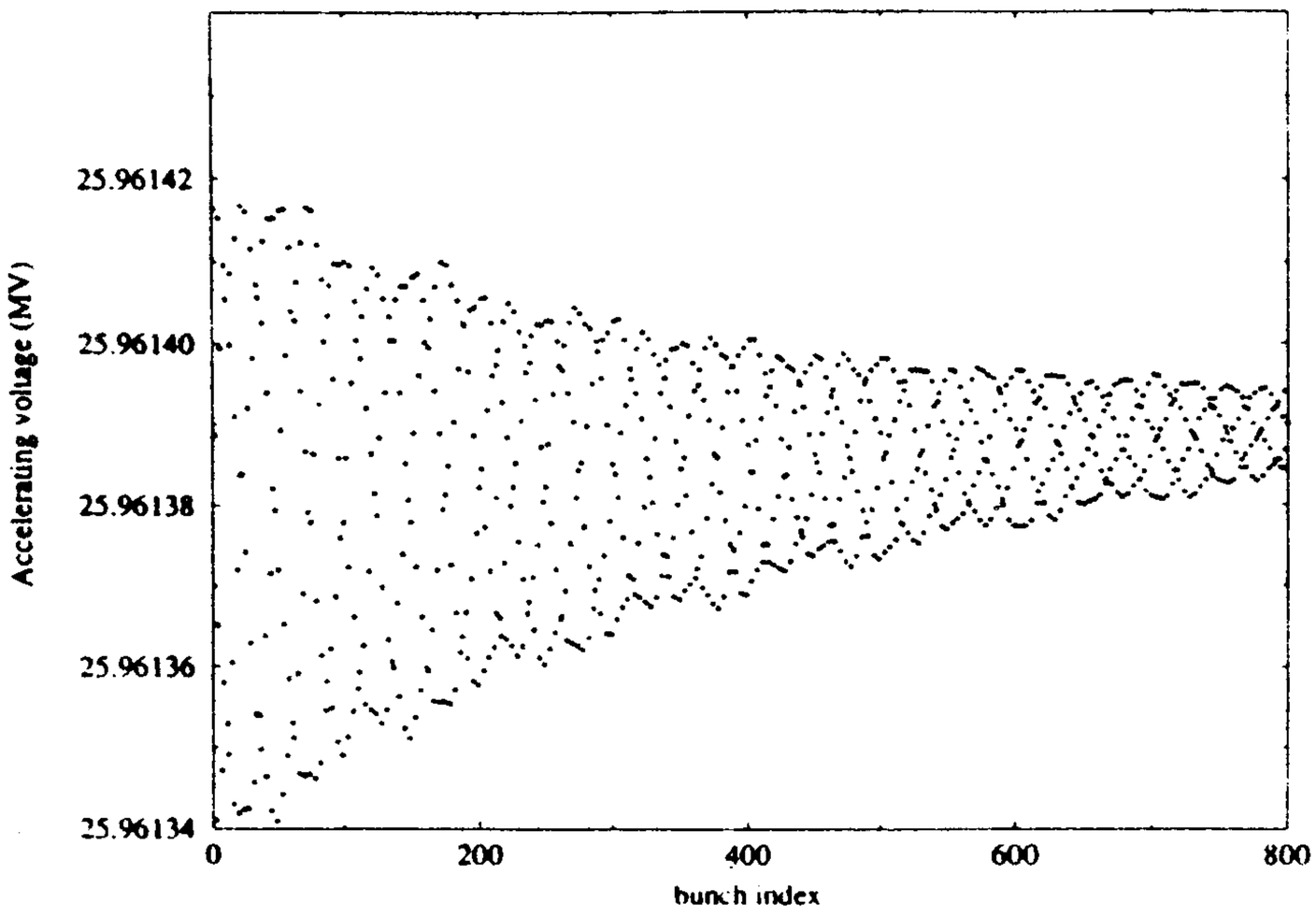

Figure 4 : Accelerating voltage evolution during 800 bunches

3. NON-RELATIVISTIC BEAM

With a non-relativistic beam however, the situation changes completely: the effects of the modes lower than the pi-mode do not cancel any more. The phase slippage occurring in the first cells, between the non relativistic beam and the lower pass-band modes, produces an effective enhancement of the shunt impedances, which is usually negligible for a relativistic beam in a well tuned cavity. Furthermore, since the beam phase is slipping all along the structure, the field jumps and the detuning due to the off-crest beam vary from cell to cell. Some appreciable fluctuation of the output energy during the beam pulse is then expected. This multi-bunch energy spread is here estimated for the SC capture cavity of the low charge injector I of the Tesla Test Facility [7].

3.a TTF Injector I

Figure 5 shows typical plots of the energy gain and the beam phase with respect to the RF wave for a single bunch going down the 9-cell capture cavity. A gradient of 10 MV/m and an injection energy of 240 KeV were assumed. Before reaching a stable value, the phase shift varies rapidly especially in the first cells.

The out of phase component of the energy transfer to the beam will thus vary along the structure, resulting in frequency detunings, which will change from cell to cell. The total frequency detuning is about 110 Hz, i.e. almost one third of the cavity bandwidth. The following table 1 points out the contribution of the different cells to the frequency detuning, with the largest detuning provided by the second cell.

1	2	3	4	5	6	7	8	9
16.2	38.5	16.5	10.1	7.15	5.15	4.23	3.4	9.3

Table 1 : Frequency detunings (in Hz) of the different cells (1 to 9)

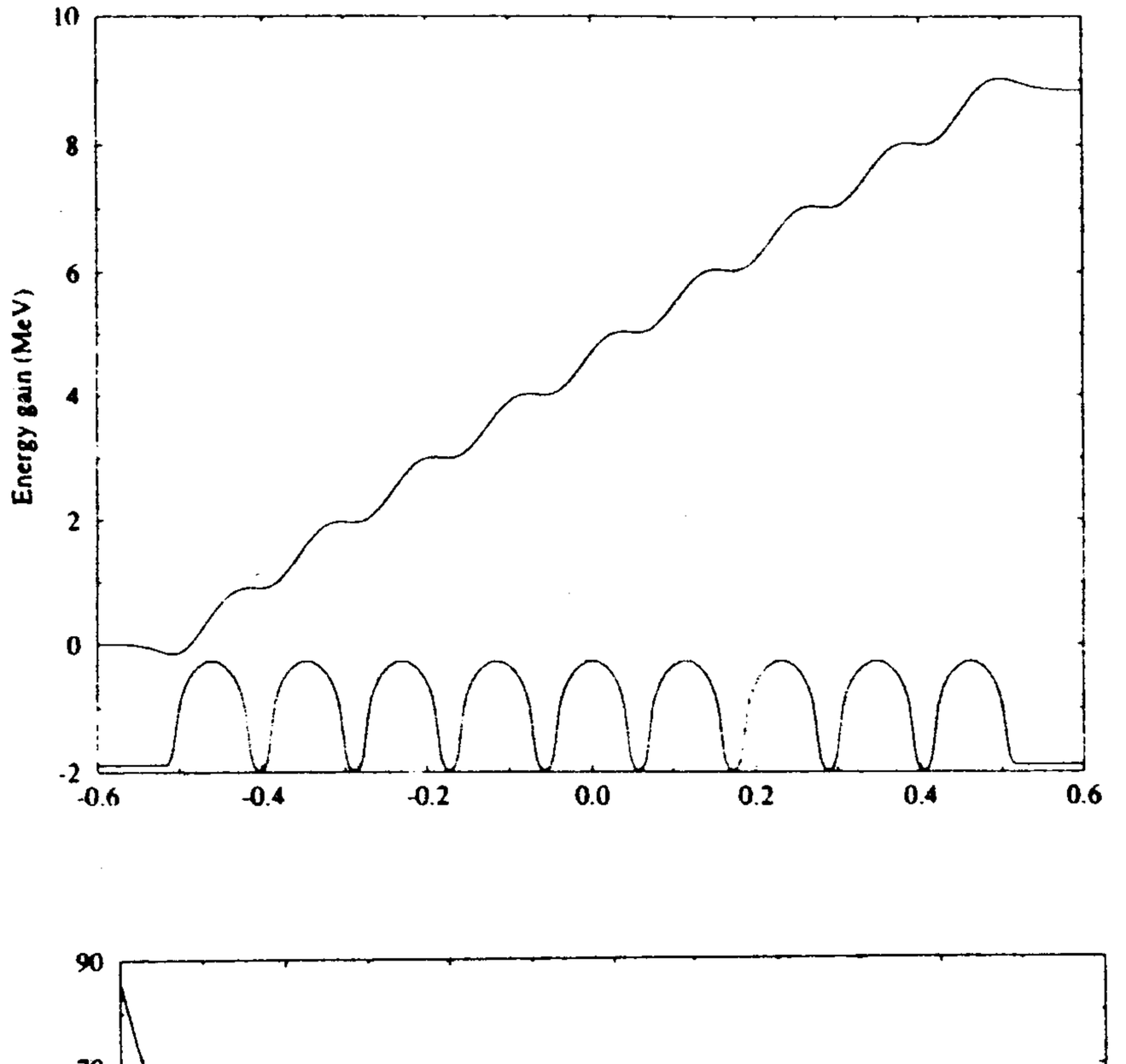

Figure 5 : Energy gain and beam phase shift along the SC capture cavity
(the cavity profile is also shown)

3.b Beam detuning compensation

When a beam is running off-crest, a cavity detuning, in addition to the critical coupling, is generally introduced [8] in order to cancel the reflected RF power and thus to minimize the RF power fed by the klystron. In the steady-state regime and for critical coupling, the tuning angle must be set to the RF phase with respect to the beam phase

$$-\tau\,\Delta\omega_\pi = \tan\psi = \tan(\phi_{rf} - \phi_b)$$

The generator and the cavity voltages are then in-phase. Furthermore, it will be shown later that this beam-detuning compensation will decrease the cavity voltage fluctuations. The phasors diagrams are drawn on Figure 6, without (a) and with (b) cavity detuning.

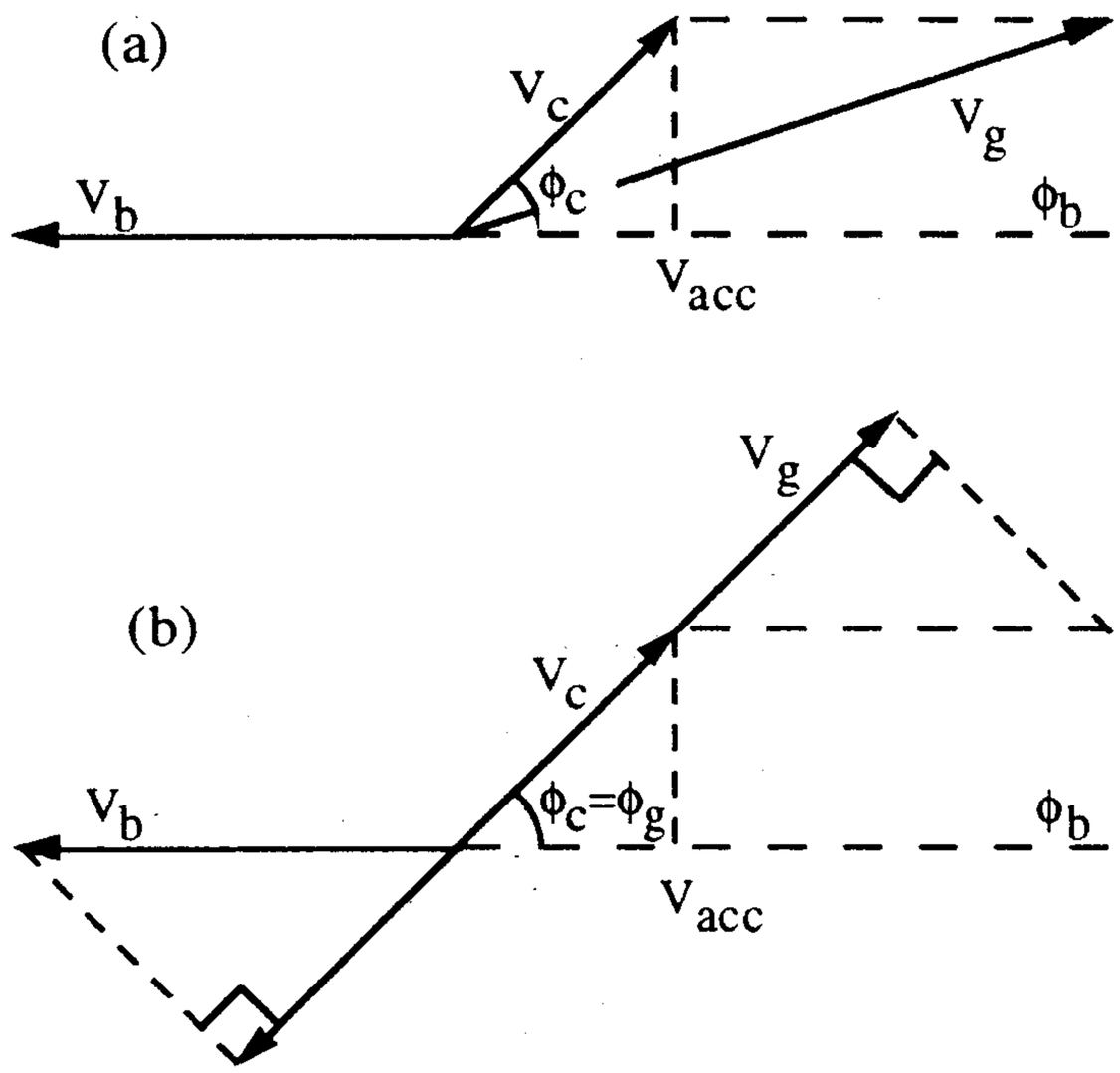

Figure 6 : Phasors diagram without (a) and with cavity detuning (b)

In order to have a constant accelerating voltage during the beam pulse, by balancing the rising generator voltage and the beam voltage, and neglecting the other modes than the pi-mode, the beam should be injected after the beginning of the RF power pulse with a delay

$t_o = \tau\, Ln\, 2$ with cavity detuning, and $t_o = \tau\, Ln \dfrac{V_g \cos\phi_g}{V_b}$ without cavity detuning.

3.c Energy Spread

The beam loading effects will differ according whether the cavity detuning is introduced or not, and also whether the power coupler is located upstream or downstream

with respect to the beam. Computations are now performed with the low charge TTF gun (bunch charge of 37 pC and bunch spacing of 4.615 ns).

Figure 7 shows the evolution of the energy gain on a short-time scale (1000 bunches), without beam detuning compensation and with the coupler linked to the in-cell or the out-cell. The accelerating voltage exhibits fluctuations with a main beating due to the nearest $8\pi/9$ mode spaced 0.76 MHz apart from the pi-mode. The shape of the oscillations is similar and the multi-bunch energy spread amounts to $9\ 10^{-4}$ in both cases.

Figure 8 shows the same plots, but with a cavity detuning of -110 Hz. The phase of the generator is assumed to track the cavity phase, at least during the field rise time. We note that the accelerating voltage fluctuations are about two times lower, giving a multi-bunch energy spread of $4\ 10^{-4}$.

Figures 9 and 10 show the accelerating voltage evolution on a longer time-scale, like the TESLA beam pulse duration of 0.8 ms (about 173 333 bunches for injector I), without and with cavity detuning. Without cavity detuning, the average compensation of the beam loading, by adjustment of the different parameters (generator, beam voltage or injection time), is not possible, resulting in a large slope on the cavity voltage at the beginning or at the end of the beam pulse. Conversely, the average compensation can be obtained when the proper cavity detuning is introduced. We note again that the voltage oscillations decay with the time constants of the other modes of the pass-band.

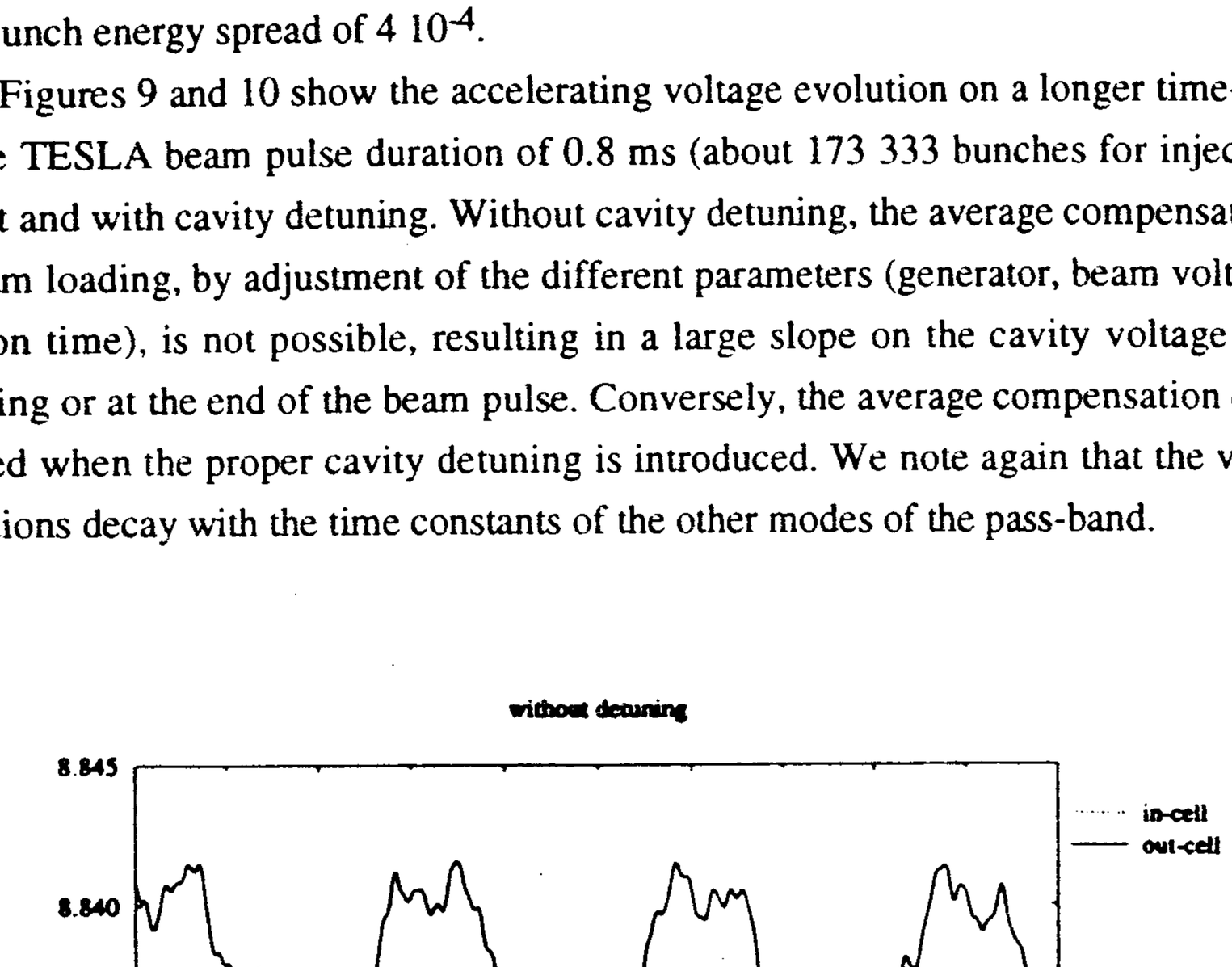

Figure 7 : Energy gain evolution without cavity detuning

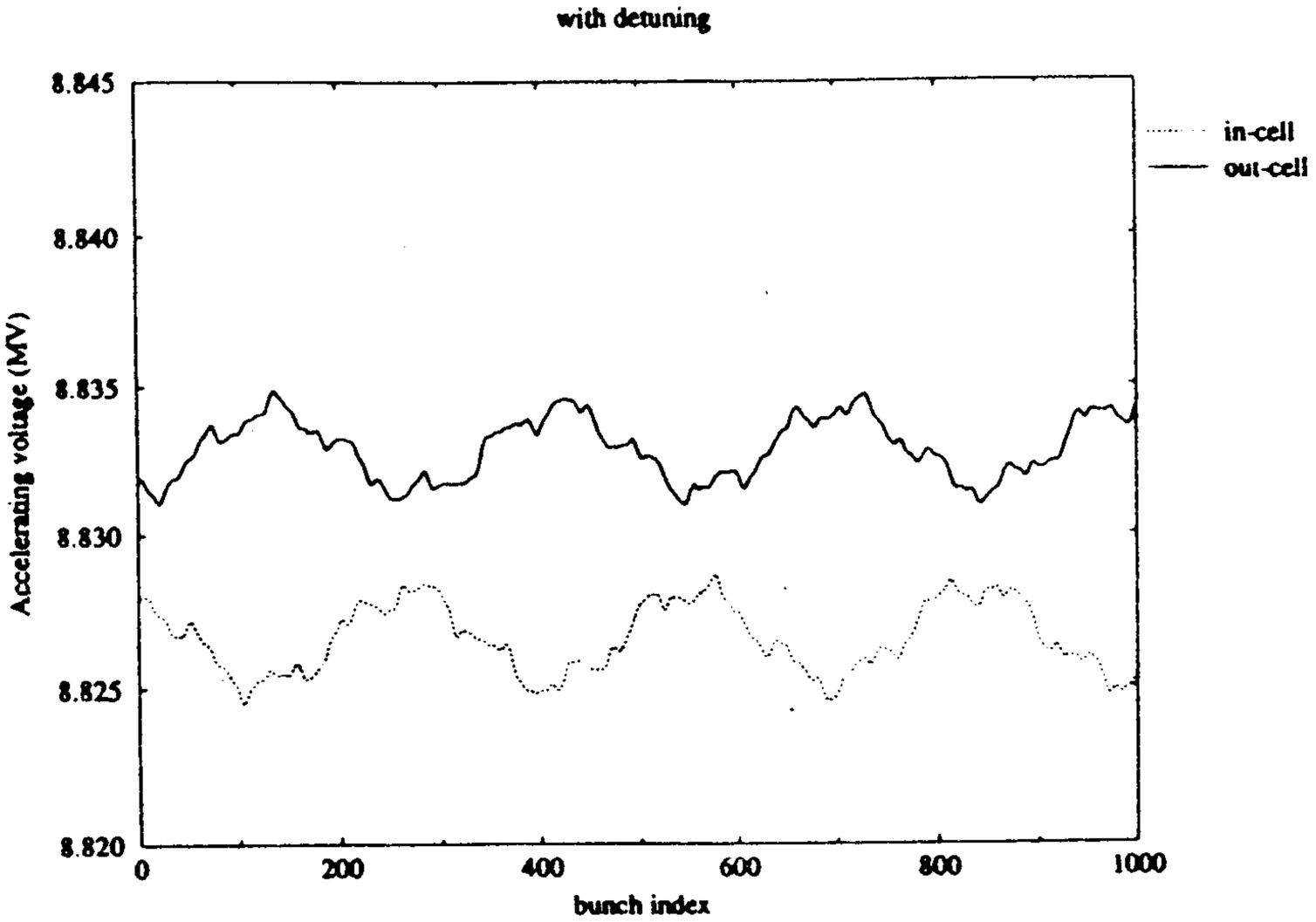

Figure 8 : Energy gain evolution with cavity detuning.

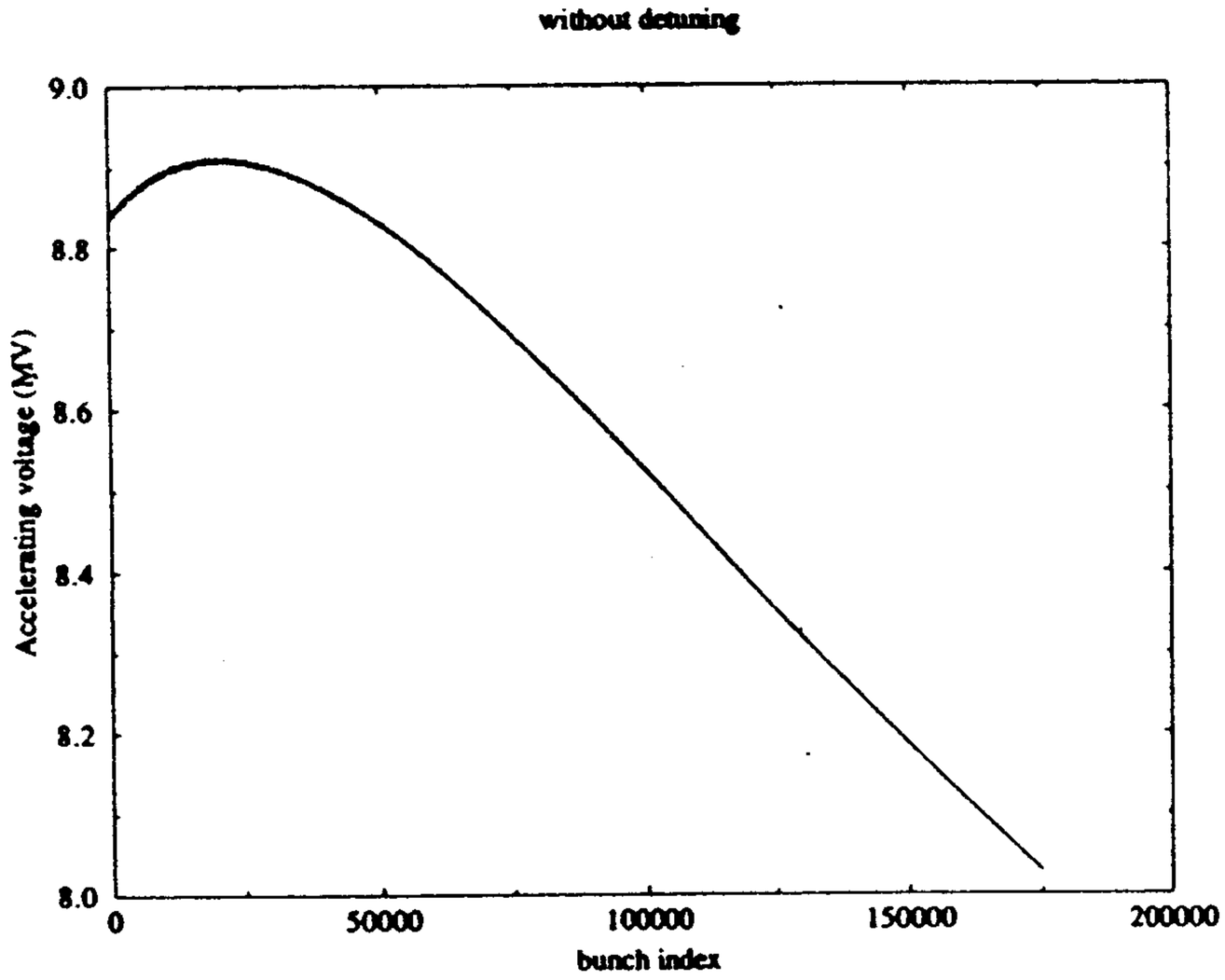

Figure 9 : Energy gain evolution on a longer time-scale (without cavity detuning).

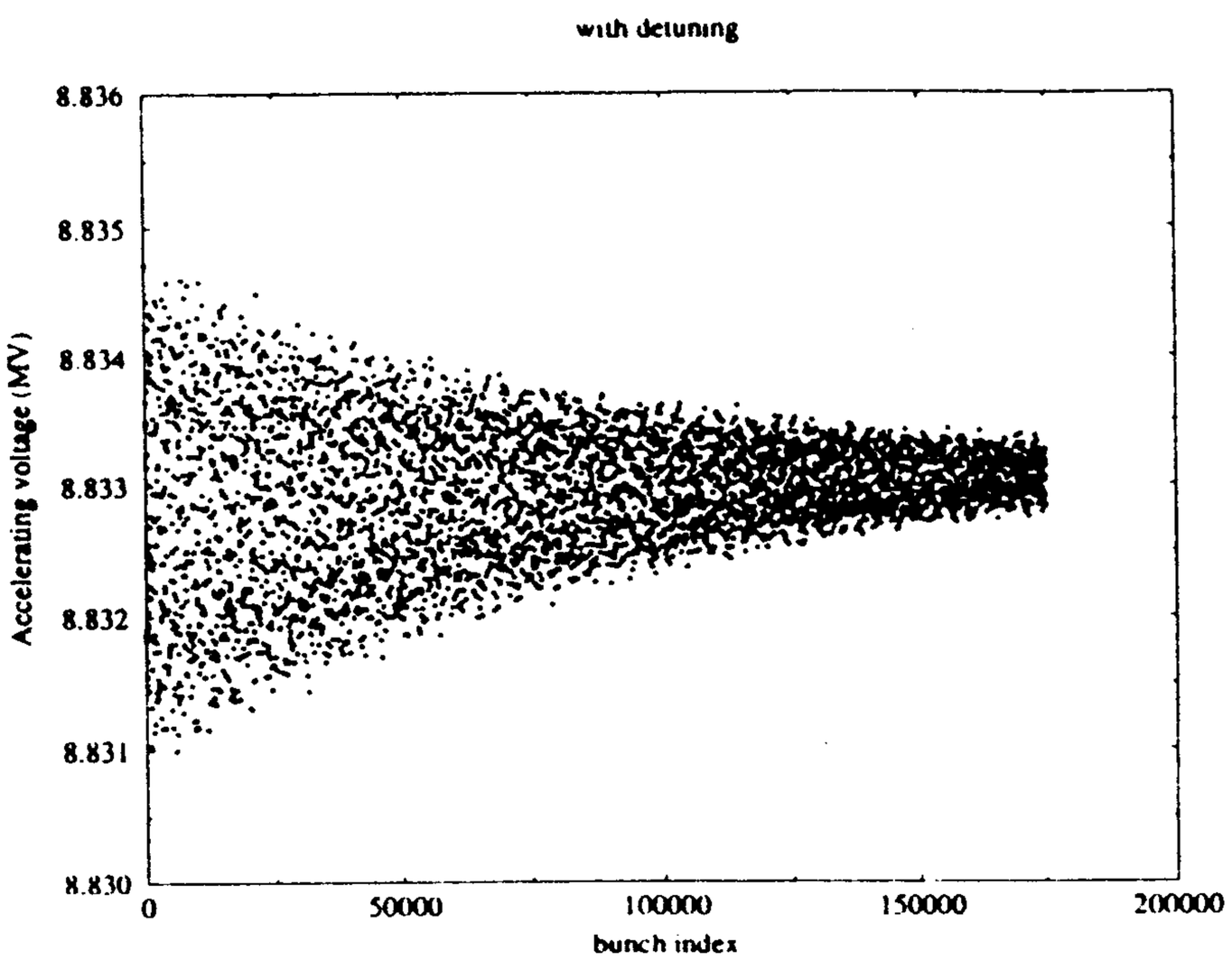

Figure 10 : Energy gain evolution on a longer time-scale (with cavity detuning).

3.d Transverse dynamics in the bunch train

We report in this paragraph some computations including space charge effects on a short time scale (1000 bunches) and without cavity detuning, (see Appendix C). Single bunch computations are shown in figure 11 at the nominal accelerating field of 10 MV/m.

As already pointed out the in the previous paragraph the dynamics of the subsequent bunches could be strongly influenced from the field propagation effects : the beating that produces energy spread affects also the other beam parameters. In figure 12-16 are shown the effects on length, radius, emittance and Twiss parameters α and β for the bunch train head (first 1000 bunches) at the exit of the capture cavity. We are concerned about this effect on a short time scale since, at longer times, a suitable cavity detuning cancels the average off-set in the energy gain and the natural damping of the lower modes occurs.

We note that the fluctuations displayed by the emittance parameters are quite small (within a few per cent).

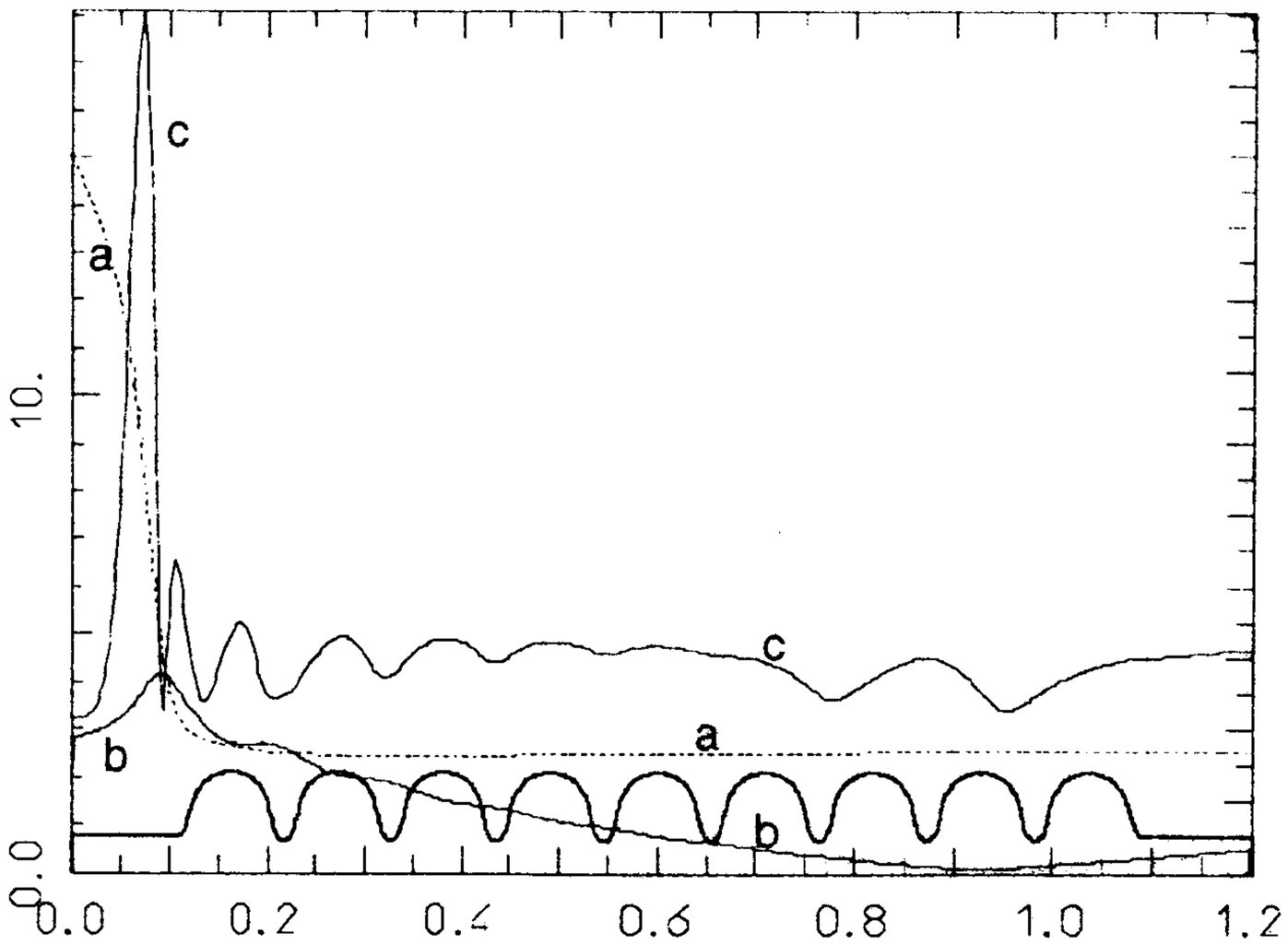

Figure 11: Single bunch computation: a-Bunch length [mm], b-Bunch radius [mm], c-rms norm. transv. emittance [mm mrad], versus z [m]

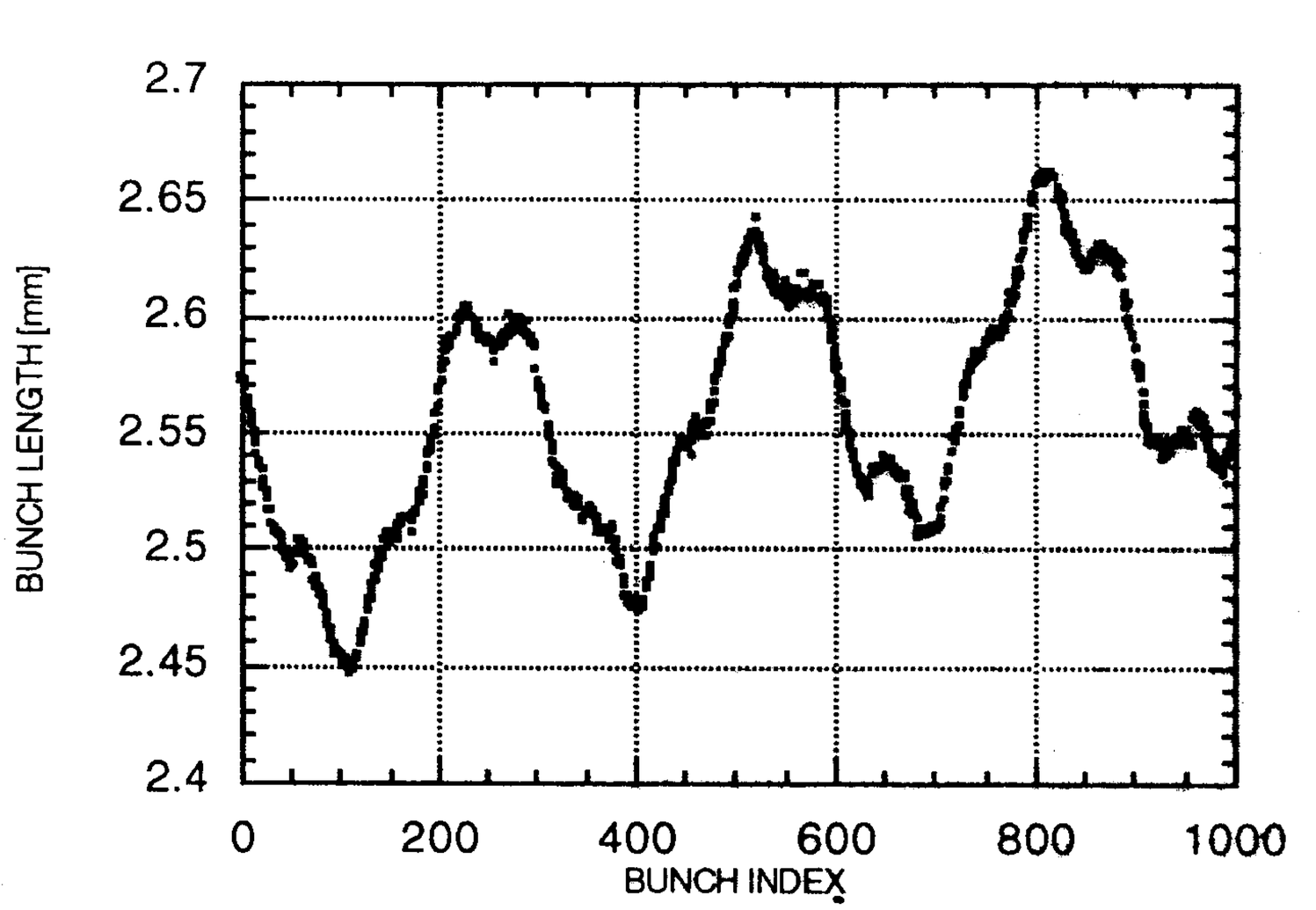

Figure 12: Bunch Length [mm]

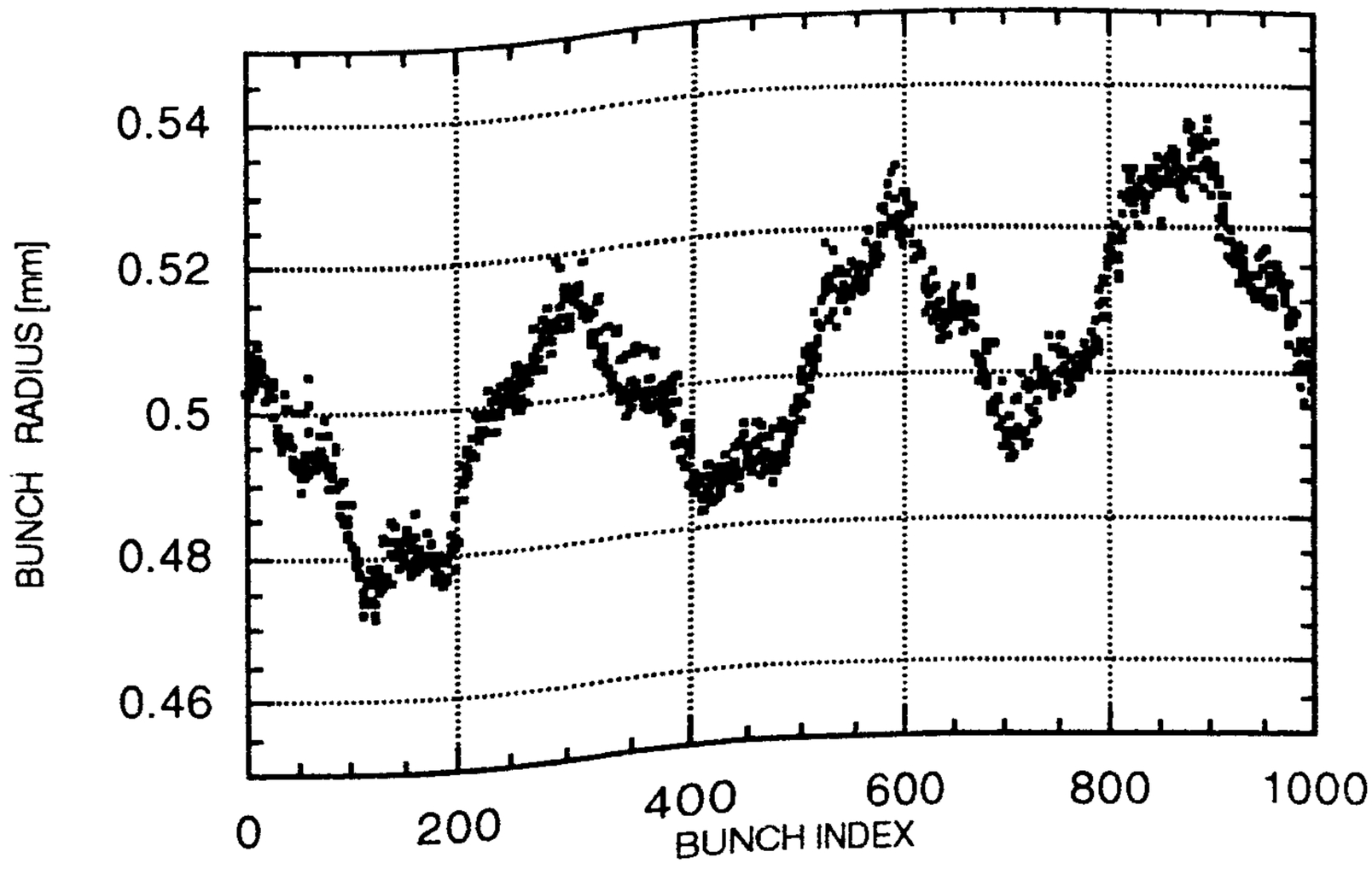

Figure 13: Bunch Radius [mm]

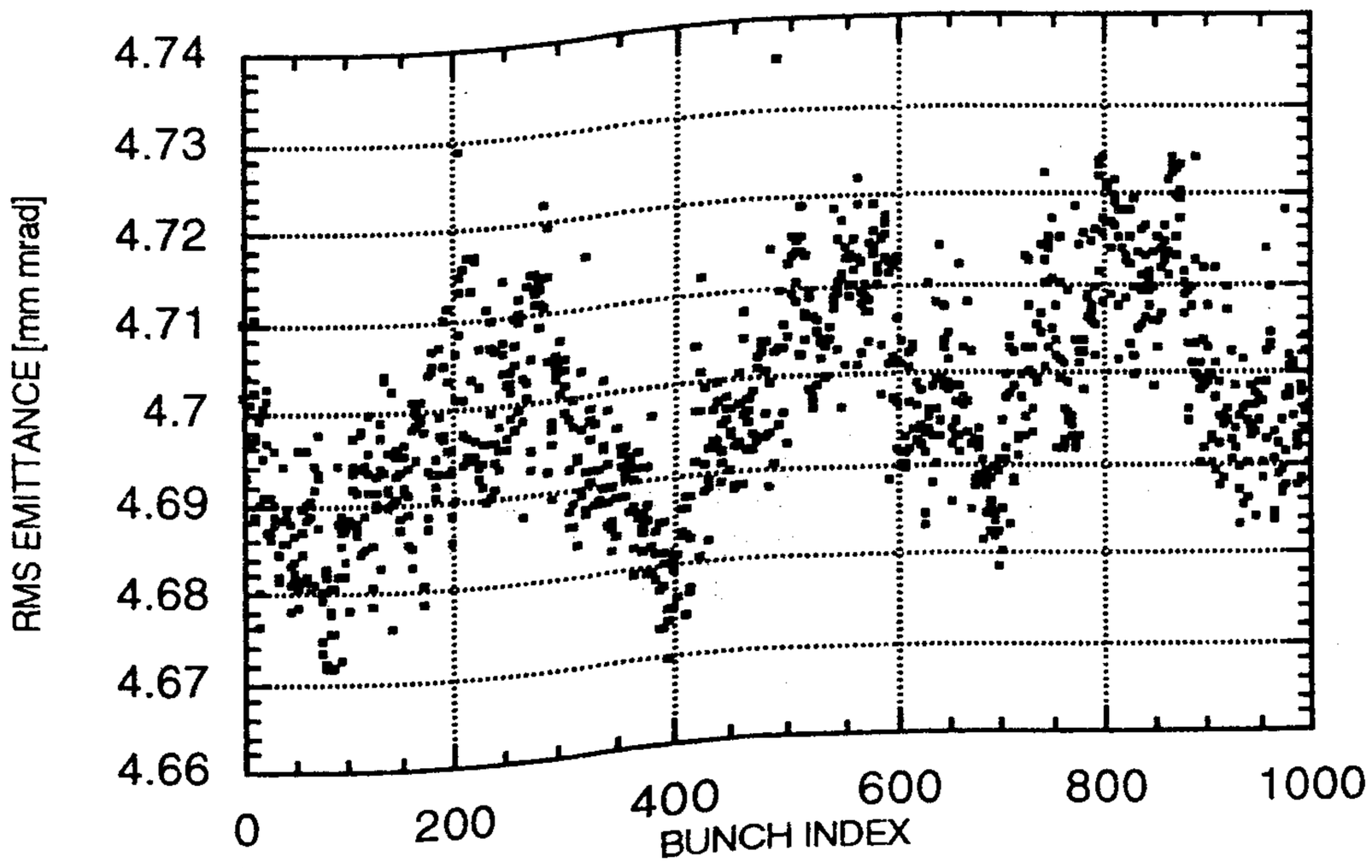

Figure 14: Rms Normalized Emittance [mm mrad]

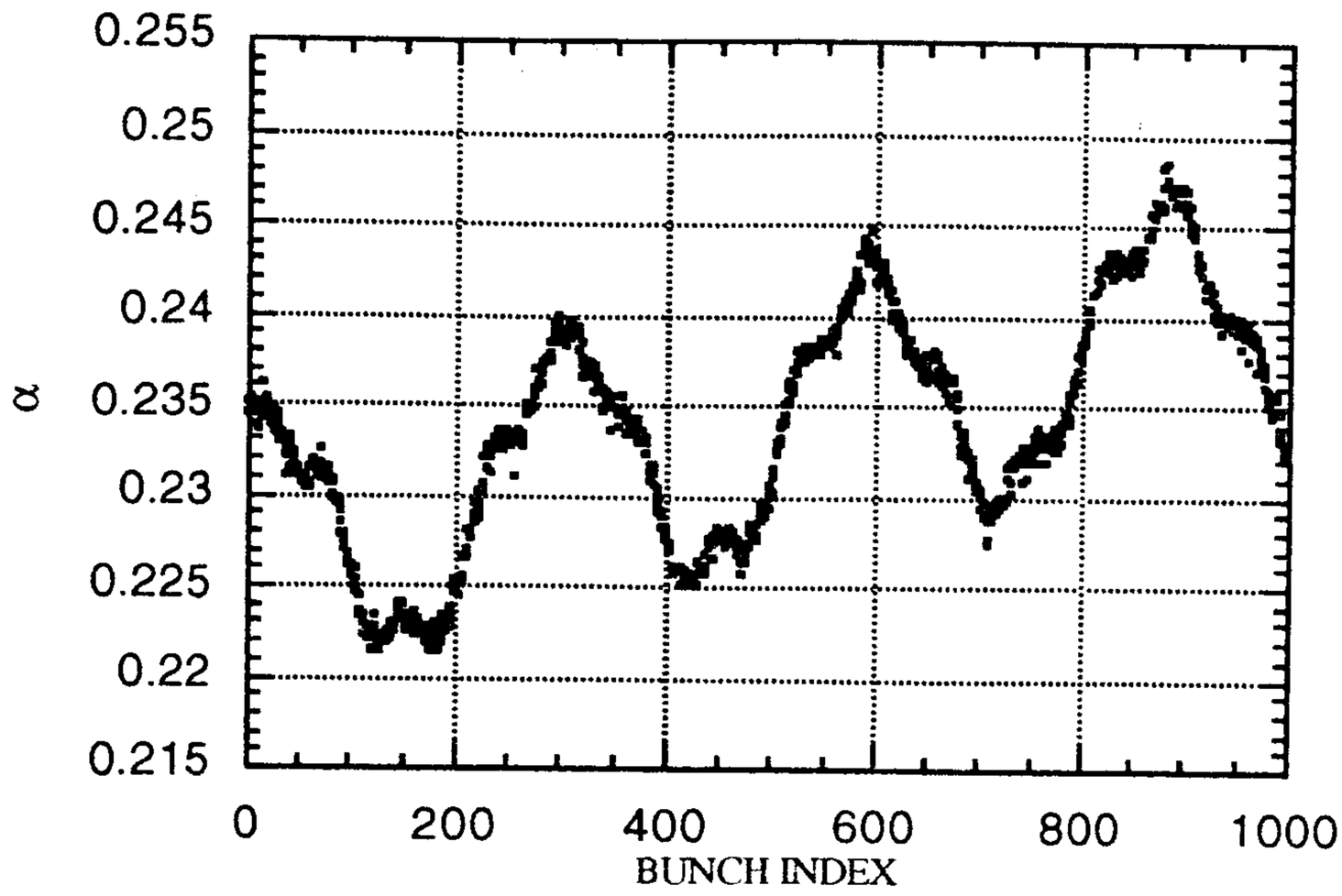

Figure 15: Twiss parameter α

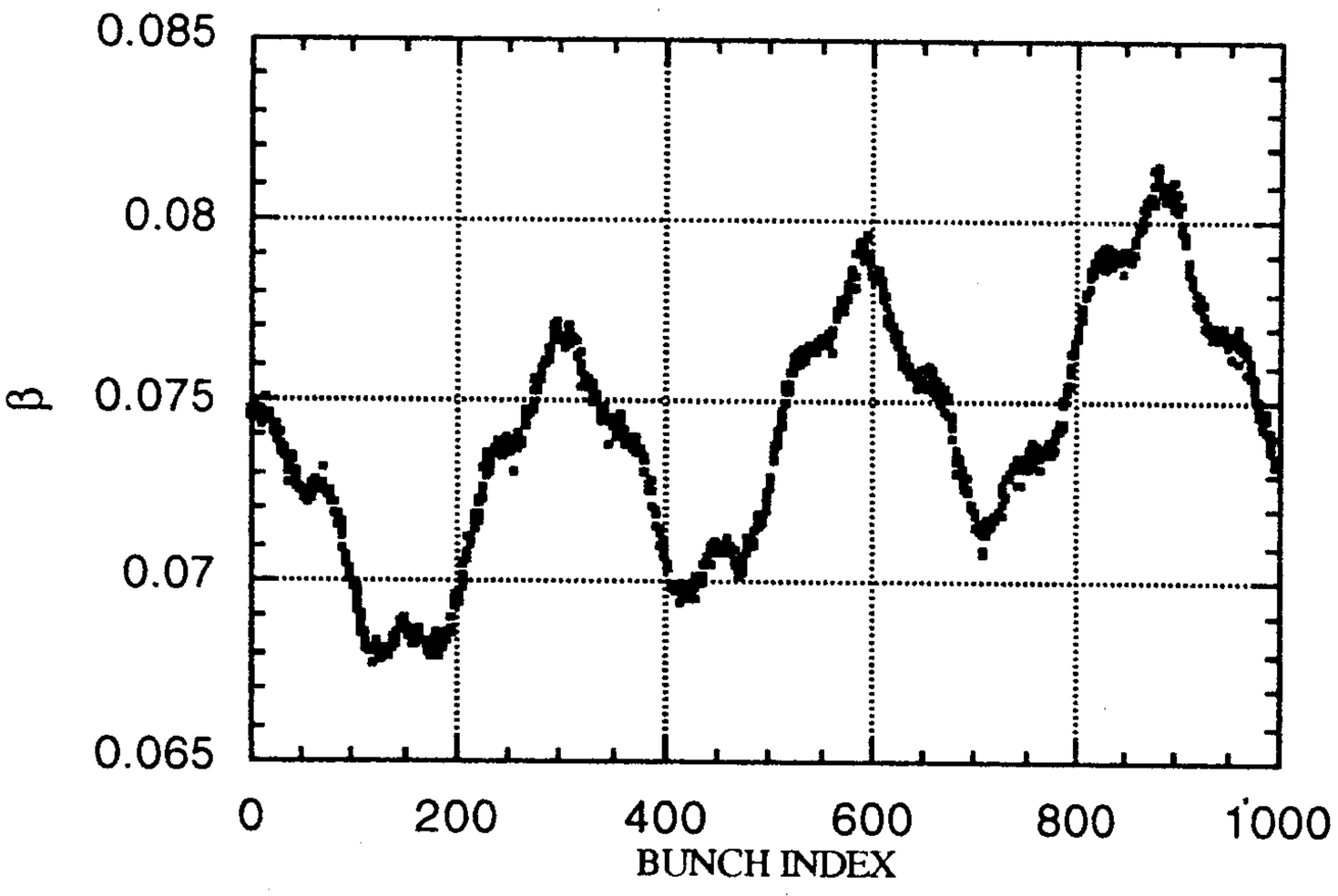

Figure 16: Twiss parameter β

4. CONCLUSION

Although the propagation effects are not harmful for a relativistic beam accelerated in a multicell cavity, they have to be taken into account with a non relativistic beam. In the latter case, the modes other than the pi-mode (especially the nearest mode) introduce larger cavity voltage beatings. For the low charge TESLA injector, the resulting bunch-to-bunch energy spread will be lower than 0.1% in any case. This value is nevertheless very small in comparison with the single-bunch energy spread of 3% , found with PARMELA simulations [7]. The impact on the transverse dynamics is also small. The TESLA cavity geometry is thus well suited to the capture section of the TTF injector. With a larger number of cells or a smaller cell-to-cell coupling, stronger effects would have been obtained. On the other hand, we could imagine larger energy spreads induced by more critical beam parameters, like the bunch charge or the input energy.

REFERENCES

[1] M. Ferrario, L. Serafini, F. Tazzioli, "Higher Order Modes Interaction with Multi-bunch Trains in Accelerating Structures", Proc. of EPAC, London, 1994, pp. 1132-1134.

[2] A. Mosnier, "Coupled Mode equations for RF Transients Calculations in Standing Wave Structures", CEA/DAPNIA/SEA 94-30, non published

[3] R.A. Jameson et al., "Design of the RF Phase and Amplitude Control System for a Proton Linear Accelerator", IEEE Trans. on Nuclear Science, June 1965.

[4] H. Henke and M. Filtz, "Envelope equations for Transients in Linear Chains of Resonators", TESLA 93-26, 1993.

[5] J. Sekutowicz, "Transient State in Standing Wave Accelerating Structures", Particle Accelerators, 1994, Vol. 45, pp. 47-58.

[6] J. C. Slater, "Microwave Electronics", 1950, D. Van Nostrand Co, New York.

[7] M. Bernard, B. Aune, S. Buhler et al., "The TESLA Test Facility Linac Injector", Proc. of EPAC, London, 1994, pp 692-694.

[8] P.B. Wilson, AIP Conf. Proc. No 87 (AIP, New York, 1982), p. 474

[9] R. M. Bevensee, "Electromagnetic Slow Wave Systems", 1964, John Wiley and Sons, Inc., New York, London, Sydney.

[10] M. Ferrario, L. Serafini, F. Tazzioli, "Multibunch beam dynamics in a superconducting linac injector", Proc. of LINAC 94, Tsukuba.

[11] M. Puglisi, "Conventional RF cavity design," CAS School, CERN 92-03, (1992).

[12] G. Mavrogenes, "Space charge effects in high current linac transport systems," ANL Report.

[13] J.D. Lawson, "The Physics of Charged Particle Beams", Oxford: Clarendon Press, 1977, pp.196

APPENDIX A - EQUIVALENT CIRCUIT OF A MULTICELL CAVITY

The multicell cavity consists of weakly coupled resonant cells (Fig.A-1). The fields in a given cell n are usually expanded in the normal modes. In the single pass-band approximation, the first monopole pass-band being very narrow compared to the width of the adjacent stop band, only a single mode can be kept from the expansion

$$E_n(\bar{r},t) = \sum_m q_n^m(t) E_{an}^m(\bar{r}) = q_n(t) E_{an}(\bar{r}) \text{ with the normalization } \int E_{an}^2 \, dV = 1$$

where $q_n(t)$ is a time function, the excitation of cell n, and $E_{an}(\bar{r})$ is the field pattern of the single mode in the cell.

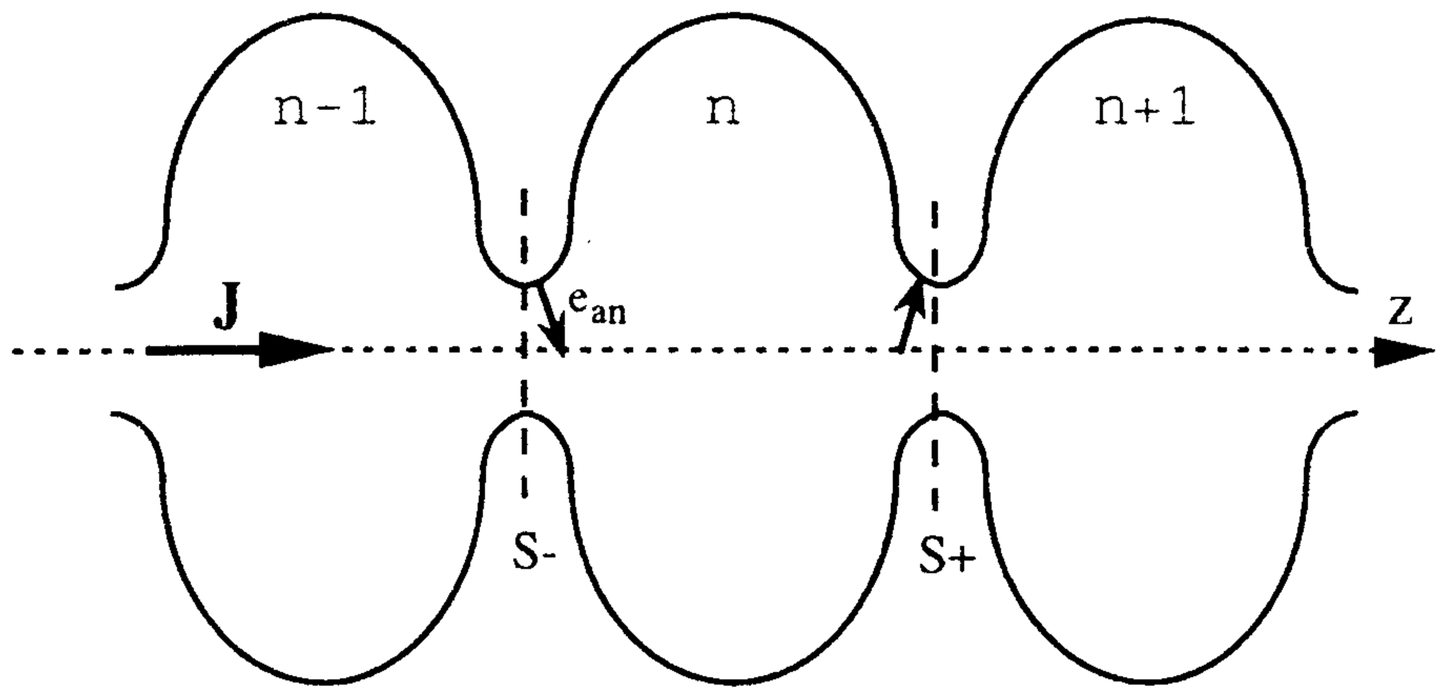

Figure A-1 : Chain of coupled resonant cells

We define the surfaces S and S' such that the tangential component of the electric field to S is zero and the tangential component of the magnetic field to S' is zero. Within the cell n, volume V_n enclosed by surface S and S', the wave equation gives the differential equation relative to the field time function q_n (Ref. [6], p. 66)

$$\frac{d^2}{dt^2} q_n(t) + \frac{\omega_o}{Q_n} \frac{d}{dt} q_n(t) + \omega_o^2 \, q_n(t) = -\omega_o \, c \int_S (\bar{n} \times E_n(\bar{r},t)) H_{an}(\bar{r}) \, dS$$
$$+ \frac{1}{\varepsilon} \frac{d}{dt} \int_S (\bar{n} \times H_n(\bar{r},t)) E_{an}(\bar{r}) \, dS - \frac{1}{\varepsilon} \frac{d}{dt} \int_{V_n} J(\bar{r},t) \, E_{an}(\bar{r}) \, dV$$

where $\bar{n}$ is a outwards normal vector to the surfaces S and S'.

There is a small tangential component of the electric field over the surface S when losses are considered (S is then the wall surface) but also when cells are coupled through small holes (S is then the hole aperture). The losses have been already included in the first member through Q_n (the weak frequency shift due to the finite Q_n has been neglected) while the integral over the coupling holes will give rise to the cell-to-cell coupling. The second term represents the applied current source of the generator and the third term represents the interaction between the beam and the cell.

The coupling integral is written explicitly by expressing properly the boundary matching of the electric field at the coupling holes, whose the tangential component is provided by the open-circuit mode e_a. For a field of even symmetry with respect to the middle plane of the cell, which is the case of the TM_{010} mode, we obtain (Ref.[9])

$$\int_S (\bar{n} \times E_n(\bar{r},t)) H_{an}(\bar{r})\, dS = \left[\frac{1}{2} q_{n-1}(t) - q_n(t) + \frac{1}{2} q_{n+1}(t)\right] \int_{S_n^-} (e_{an} \times H_{an}) \bar{i}_z \, dS$$

where S_n^- is the integration surface of the first coupling aperture of the cell n.

We define the coupling factor K, independent on the cell n

$$2K = -\frac{c}{\omega_o} \int_{S_n^-} (e_{an} \times H_{an}) \bar{i}_z \, dS$$

The differential equation relative to the cell n is then

$$\frac{d^2}{dt^2} q_n(t) + \frac{\omega_o}{Q_n} \frac{d}{dt} q_n(t) + \omega_o^2 \, q_n(t) = 2K\omega_o^2 \left[\frac{1}{2} q_{n-1}(t) - q_n(t) + \frac{1}{2} q_{n+1}(t)\right]$$
$$+ \frac{1}{\varepsilon} \frac{d}{dt} \int_S (\bar{n} \times H_n(\bar{r},t)) E_{an}(\bar{r})\, dS - \frac{1}{\varepsilon} \frac{d}{dt} \int_{V_n} J(\bar{r},t)\, E_{an}(\bar{r})\, dV$$

We rewrite this dispersive equation of cell n, driven by a generator current and a beam current

$$-K\, q_{n-1}(t) + (1+2K) q_n(t) - K\, q_{n+1}(t) = -\frac{1}{\omega_o^2} \frac{d^2}{dt^2} q_n(t) - \frac{1}{Q_n \omega_o} \frac{d}{dt} q_n(t)$$
$$+ \frac{1}{\varepsilon \omega_o^2} \frac{d}{dt} \int_S (\bar{n} \times H_n(\bar{r},t)) E_{an}(\bar{r})\, dS - \frac{1}{\varepsilon \omega_o^2} \frac{d}{dt} \int_{V_n} J(\bar{r},t)\, E_{an}(\bar{r})\, dV$$

The intrinsic losses of the cells are represented by Q_o , β_n is the coupling of cell n to an external circuit and Q_n is the loaded Q of cell n. For a multicell driven by the first cell

$$\text{for} \quad n \neq 1 \quad Q_n = Q_o$$
$$\text{for} \quad n = 1 \quad Q_1 = Q_o / (1+\beta_1)$$

By making the following substitutions

$$V_n(t) = q_n(t) \quad K = L / L_k \quad LC\omega_o^2 = 1$$
$$Q_o = R_o C \omega_o = R_o / (L\omega_o) = Q_n(1+\beta_n)$$

we obtain the equations of the equivalent circuit (figure A-2) for fields of even symmetry where $V_n(t)$ is now the voltage of the resonator n

$$-K\,V_{n-1}(t)+(1+2K)\,V_n(t)-K\,V_{n+1}(t)=-\frac{1}{\omega_o^2}\frac{d^2}{dt^2}V_n(t)-\frac{1}{Q_n\omega_o}\frac{d}{dt}V_n(t)$$
$$+L\frac{d}{dt}I_{gn}-L\frac{d}{dt}I_{bn}$$

with the generator and beam currents given by

$$I_{gn}=\frac{C}{\varepsilon}\int_S(\bar{n}\times H_n(\bar{r},t))E_{an}(\bar{r})\,dS$$

$$I_{bn}=\frac{C}{\varepsilon}\int_{V_n}J(\bar{r},t)\,E_{an}(\bar{r})\,dV$$

While the beam current term is valid for all cells, the generator current term exists only for the first cell. The impedance of the generator must be added to the first cell side. In addition, An inductance equal to the half coupling inductance has been added at both ends of the circuit in order to get the so-called flat pi-mode, when the excitation is the same in all the cells in the steady-state regime.

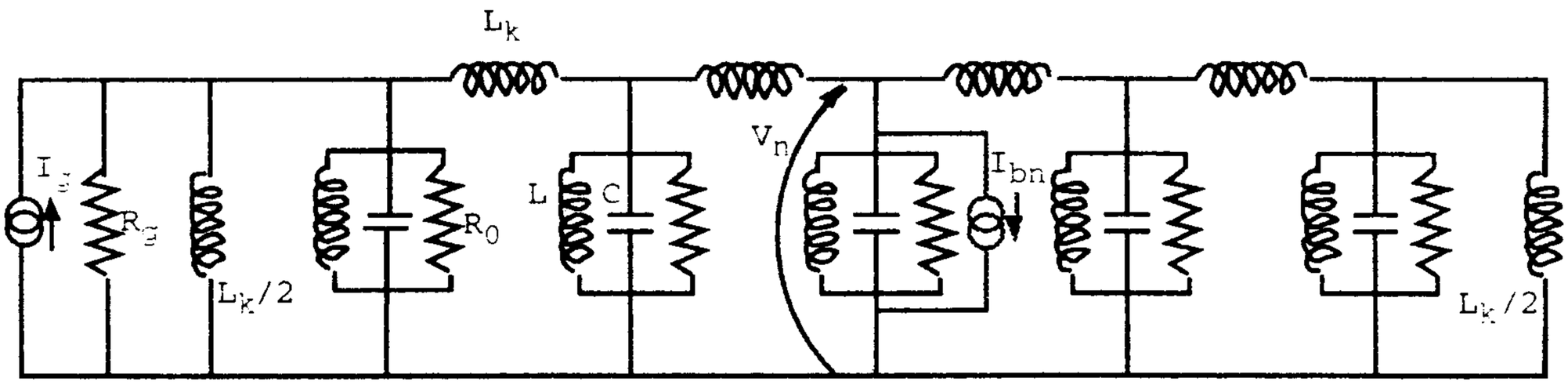

Figure A-2 : Equivalent circuit (with lumped elements in parallel)

We define the generator and beam voltages $V_{gn}=\frac{R_o}{1+\beta_n}I_{gn}\quad V_{bn}=\frac{R_o}{1+\beta_n}I_{bn}$

With the new notations, the mesh equations of the equivalent circuit are finally

for the first cell

$$(1+3K)\,V_1(t)-K\,V_2(t)=-\frac{1}{\omega_o^2}\frac{d^2}{dt^2}V_1(t)-\frac{1}{Q_1\omega_o}\frac{d}{dt}V_1(t)-\frac{1}{Q_1\omega_o}\frac{d}{dt}V_{b1}(t)+\frac{1}{Q_1\omega_o}\frac{d}{dt}V_g(t)$$

for the cell index n

$$-K\,V_{n-1}(t)+(1+2K)\,V_n(t)-K\,V_{n+1}(t)=-\frac{1}{\omega_o^2}\frac{d^2}{dt^2}V_n(t)-\frac{1}{Q_o\omega_o}\frac{d}{dt}V_n(t)-\frac{1}{Q_o\omega_o}\frac{d}{dt}V_{bn}(t)$$

for the last cell N

$$-K\,V_{N-1}(t)+(1+3K)\,V_N(t)=-\frac{1}{\omega_o^2}\frac{d^2}{dt^2}V_N(t)-\frac{1}{Q_o\omega_o}\frac{d}{dt}V_N(t)-\frac{1}{Q_o\omega_o}\frac{d}{dt}V_{bN}(t)$$

APPENDIX B - MODAL ANALYSIS OF THE PASS-BAND

The dispersive equations governing the time-dependent excitation of the cells, driven by a beam source and a generator in the first cell, can be written in a matrix notation

$$\mathbf{A}\,\mathbf{V} = -\frac{1}{\omega_o^2}\,\ddot{\mathbf{V}} - \mathbf{B}\,\dot{\mathbf{V}} - \mathbf{B}\,\dot{\mathbf{V}}_\mathbf{b} + \mathbf{B}\,\dot{\mathbf{V}}_\mathbf{g} \qquad \text{(B-1)}$$

where $\mathbf{V}$, $\mathbf{V_b}$ and $\mathbf{V_g}$ are a column vectors giving the excitation of the cells, the beam induced voltage and the generator voltage, respectively.

$$\mathbf{V} = \begin{bmatrix} V_1 \\ V_2 \\ \vdots \\ V_N \end{bmatrix} \qquad \mathbf{V_b} = \begin{bmatrix} V_{b1} \\ V_{b2} \\ \vdots \\ V_{bN} \end{bmatrix} \qquad \mathbf{V_g} = \begin{bmatrix} V_g \\ 0 \\ \vdots \\ 0 \end{bmatrix}$$

A and **B** are square matrices with the dimension N, the number of cells

$$\mathbf{A} = \begin{bmatrix} 1+3K & -K & & & \\ -K & \ddots & \ddots & & \mathbf{0} \\ & -K & 1+2K & -K & \\ & & \ddots & \ddots & -K \\ & \mathbf{0} & & -K & 1+3K \end{bmatrix} \qquad \mathbf{B} = \begin{bmatrix} 1/(Q_1\omega_o) & 0 & \cdots & \\ 0 & 1/(Q_o\omega_o) & & \\ \vdots & & \ddots & \\ & & & 1/(Q_o\omega_o) \end{bmatrix}$$

The second order matrix equation B-1 can be solved by standard algebra, after transformation into first order matrix equations. Instead of that, we prefer to look for the matrix equation involving the usual modes found by solving the steady-state homogenous system. These steady-state modes are moreover computed by cavity codes like Urmel. For that purpose, we have to diagonalize the matrix **A**. We take the transformation matrix **T**, such that $\mathbf{V} = \mathbf{T}\,\mathbf{Z}$. The system B-1 can be then written

$$\mathbf{T}^{-1}\mathbf{A}\,\mathbf{T}\,\mathbf{Z} = -\frac{1}{\omega_o^2}\,\ddot{\mathbf{Z}} - \mathbf{T}^{-1}\mathbf{B}\,\dot{\mathbf{V}} - \mathbf{T}^{-1}\mathbf{B}\,\dot{\mathbf{V}}_\mathbf{b} + \mathbf{T}^{-1}\mathbf{B}\,\dot{\mathbf{V}}_\mathbf{g} \qquad \text{(B-2)}$$

The transformation matrix is the modal matrix if the matrix $\Lambda = \mathbf{T}^{-1}\mathbf{A}\,\mathbf{T}$ is diagonal. The diagonal elements of Λ are the eigenvalues of **A**

$$\Lambda = \begin{bmatrix} \lambda_1 & & & \\ & \ddots & 0 & \\ & & \lambda_m & \\ & 0 & & \ddots \\ & & & & \lambda_N \end{bmatrix} \quad \text{with} \quad \lambda_m = \frac{\omega_m^2}{\omega_o^2} = 1 + 2K(1 - \cos\frac{m\pi}{N})$$

The column vectors of the modal matrix are the eigenvectors

$$\begin{bmatrix} V_1 \\ \vdots \\ V_n \\ \vdots \\ V_N \end{bmatrix} = \begin{bmatrix} T_{11} & T_{12} & \cdots & & T_{1N} \\ \vdots & & & & \\ T_{n1} & \cdots & T_{nm} & \cdots & T_{nN} \\ \vdots & & & & \vdots \\ T_{N1} & & & & T_{NN} \end{bmatrix} \begin{bmatrix} Z_1 \\ \vdots \\ Z_n \\ \vdots \\ Z_N \end{bmatrix} \quad \text{with} \quad T_{nm} = c_m \sin\,(n - \frac{1}{2})\frac{m\pi}{N}$$

The constant c_m is chosen with the normalization $\sum_n T_{nm}^2 = N$, while the eigenvectors belonging to different eigenvalues are orthogonal $\sum_n T_{nm} T_{nk} = 0 \quad \text{for} \quad m \neq k$

The inverse matrix is then given by the transpose matrix $\mathbf{T}^{-1} = \frac{1}{N}\mathbf{T}^t$

The excitation of the cell n is now expressed in terms of the modes m : $V_n = \sum_m T_{nm} Z_m$

Performing the matrix multiplications of equation B-2, we find for the differential equation relative to the mode m (row m of the system))

$$\lambda_m Z_m = -\frac{1}{\omega_o^2}\ddot{Z}_m - \sum_n \frac{T_{nm}}{NQ_n\omega_o}\dot{V}_n + \frac{T_{1m}}{NQ_1\omega_o}\dot{V}_g - \sum_n \frac{T_{nm}}{NQ_n\omega_o}\dot{V}_{bn}$$

We replace the excitation of cell n by $V_n = \sum_k T_{nk} Z_k$, and rearrange the terms

$$\ddot{Z}_m + \sum_{n,k} T_{nm} T_{nk} \frac{\omega_o}{NQ_n}\dot{Z}_k + \omega_m^2 Z_m = T_{1m}\frac{\omega_o}{NQ_1}\dot{V}_g - \sum_n T_{nm}\frac{\omega_o}{NQ_n}\dot{V}_{bn}$$

We note that the modes are coupled through the damping term. After substitution of the Q_n expressions for a multicell driven by the first cell

$$\text{for} \quad n \neq 1 \quad Q_n = Q_o$$
$$\text{for} \quad n = 1 \quad Q_1 = Q_o / (1 + \beta_1)$$

the damping term becomes

$$\sum_{n,k} T_{nm} T_{nk} \frac{\omega_o}{NQ_n}\dot{Z}_k = \frac{\omega_o}{NQ_o}\sum_{n,k} T_{nm} T_{nk}\dot{Z}_k + T_{1m}\frac{\beta_1\omega_o}{NQ_o}\sum_k T_{1k}\dot{Z}_k$$

The first term represents the well-known mode coupling from wall losses while the second term represents the mode coupling from the external Q of the first drive cell. However, because of the orthogonality property of the eigenvectors, the intermode coupling due to wall losses vanishes when we consider the modes of a single pass-band

$$\sum_n T_{nm} T_{nk} = 0 \quad \text{for} \quad m \neq k$$

and only the intermode coupling due to the first drive cell is relevant. The damping term amounts finally to

$$\sum_{n,k} T_{nm} T_{nk} \frac{\omega_o}{N Q_n} \dot{Z}_k = \frac{\omega_o}{Q_o} \dot{Z}_m + T_{1m} \frac{\omega_o}{Q_{ex}} \sum_k T_{1k} \dot{Z}_k$$

where $Q_{ex} = \dfrac{N Q_o}{\beta_1}$ is the global external Q of the multicell cavity for the pi-mode.

The m[th] differential equation is then

$$\ddot{Z}_m + \frac{\omega_o}{Q_o} \dot{Z}_m + T_{1m} \frac{\omega_o}{Q_{ex}} \sum_k T_{1k} \dot{Z}_k + \omega_m^2 Z_m = T_{1m} \frac{\omega_o}{N Q_1} \dot{V}_g - \sum_n T_{nm} \frac{\omega_o}{N Q_n} \dot{V}_{bn}$$

We replace the beam voltages by the current sources $I_{bn} = V_{bn} / R_n$, and we use the property of the inverse matrix, by transforming the beam interaction with the individual cells to the beam interaction with the mode m

$$\ddot{Z}_m + \frac{\omega_o}{Q_o} \dot{Z}_m + T_{1m} \frac{\omega_o}{Q_{ex}} \sum_k T_{1k} \dot{Z}_k + \omega_m^2 Z_m = T_{1m} \frac{\omega_o}{N Q_1} \dot{V}_g - \frac{1}{C} \dot{I}_{bm}$$

Substituting the original expressions of the generator and beam voltages, we obtain

$$\begin{aligned} \ddot{Z}_m + \frac{\omega_o}{Q_o} \dot{Z}_m + T_{1m} \frac{\omega_o}{Q_{ex}} \sum_k T_{1k} \dot{Z}_k + \omega_m^2 Z_m = {} & \frac{T_{1m}}{N\varepsilon} \frac{d}{dt} \int_S (\bar{n} \times H_n(\bar{r},t)) E_{an}(\bar{r})\, dS \\ & - \frac{1}{\varepsilon} \frac{d}{dt} \int_{V_{cav}} J(\bar{r},t)\, E_a^m(\bar{r})\, dV \end{aligned} \qquad \text{(B-3)}$$

where the beam interaction term has to be integrated along the whole cavity.

Once the evolution of the time functions z_m is found, the excitation of cell n and the net field along the cavity are given by summations on these modes

$$q_n(t) = \sum_m T_{nm}\, z_m(t) \qquad E(\bar{r},t) = \sum_m z_m(t)\, E_a^m(\bar{r})$$

Field envelopes - During the field rise time or between two bunch passages, the modes are just driven by the generator through the end-cell. In addition, when superconducting cavities are considered, the external coupling is high ($Q_o >> Q_{ex}$) The differential equation (B-3), relative to mode m, can then be written

$$\ddot{Z}_m + \frac{2}{\tau_m}\sum_k T_{1k}\dot{Z}_k + \omega_m^2 Z_m = \frac{2}{\tau_m}\dot{V}_g \qquad \text{(B-4)}$$

where we defined a RF time constant τ_m for the mode m

$$\tau_m = \frac{2Q_m}{\omega_m} \approx \frac{1}{T_{1m}}\frac{2Q_{ex}}{\omega_m}$$

We note this evidence that the more the excitation of the mode in the drive cell T_{1m} is large, the more the loaded Q of this mode is small. Driven by a RF generator and the beam current, the time field function will oscillate also at high frequency. Since we are interested in the envelope equations, we define amplitudes and phases for all quantities

$z_m = A_m\, e^{j\phi_m} \times e^{j\omega_r t}$ for the excitation of the mode m

$V_g = A_g\, e^{j\phi_g} \times e^{j\omega_r t}$ for the generator voltage

where all the phases have been defined with respect to a reference frequency ω_r, generally fixed by the beam. Assuming slow amplitude and phase variations on the time scale of the RF period, it is straightforward to transform the second order differential equations of (B-4) into first order ones. The evolution of the amplitude and phase envelopes is then given by a system of first order equations

$$\tau_m\left[\dot{A}_m + j\left(\dot{\phi}_m + \Delta\omega_m\right)\right] e^{j\phi_m} + \sum_k T_{1k}A_k\, e^{j\phi_k} = A_g\, e^{j\phi_g} \qquad \text{(B-5)}$$

where $\Delta\omega_m = \omega_r - \omega_m$, is the frequency deviation between the resonance of the mode m and the reference frequency.

Separating real and imaginary parts, we obtain a system of 2N coupled differential equations of first order, which can be easily numerically integrated. The excitation of cell n of the cavity is obtained from a summation on the modes of the pass-band

$$V_n = \sum_m T_{nm}\, z_m = \sum_m T_{nm}\, A_m\, e^{j\phi_m} \times e^{j\omega_r t}$$

Beam interaction - The longitudinal motion of the injected particles is calculated by numerical integration along the accelerating structure. The phase variation of a particle i during the transit time and the net voltage gain for vanishing space charge are given by

$$\frac{d\phi_i}{dz} = \frac{\omega_r}{c\beta_i(z)} \qquad \frac{dV_i^{acc}}{dz} = E_{(z,t)}^{c.m.f.} = E(z,t)\, e^{j\phi_i(z)} = \sum_m A_m\, E_a^m(z)\, e^{j(\phi_i(z)+\phi_m)}$$

where all phases have been defined at a reference plane (the cavity entrance for example). The space charge effects, which have been neglected in the previous equations, can be added when the bunch charge is not so small [1].
On the other hand, the particle i produces the RF current (N_p is the number of particles per bunch and I_o is the dc current during the beam pulse)

$$I_i(z,t) = \frac{2I_o}{N_p}\, e^{-j\phi_i(z)} \times e^{j\omega_r t}$$

The beam interaction integrals of the equation (B-3) can then be computed

$$-\frac{1}{\varepsilon}\frac{d}{dt}\int_{V_{cav}} J(\vec{r},t)\, E_a^m(\vec{r})\, dV = -\frac{j\omega_r}{\varepsilon}\frac{2I_o}{N_p}\int_{cav} e^{-j\phi_i(z)}\, E_a^m(z)\, dz \times e^{j\omega_r t}$$

They will generate amplitude and phase jumps in the excitation z_m of the mode m during each bunch transit.

APPENDIX C - THE HOMDYN MODEL

A fast running code (HOMDYN) has been developed to deal with the evolution of high charge, not fully relativistic electron bunches in RF fields of an accelerating cavity, taking into account the field induced by the beam in the fundamental and higher order modes, and the variation of bunch sizes due to both the RF fields and space charge. It has been tested by comparing single bunch results with that of ITACA [1] and PARMELA [10]

We use a current density description of the beam and slowly varying envelope approximation (SVEA) for the evolution of the cavity normal modes. Motion and field equations are coupled together through the driving current term.

The code allows to follow the evolution of both the longitudinal and transverse envelopes of each bunch in a train. By slicing the bunch in an array of cylinders, each subject to the local fields, one obtains also the energy spread and the emittance degradation due to phase correlation of RF and space charge effects. The present version deals only with TM monopole modes.

Because of the long interaction time the field equations require also an excitation term represented by an on axis localized generator in order to take into account the cavity re-filling from bunch to bunch passage.

THE FIELD EQUATIONS:

We represent the electric field in the cavity as a sum of normal orthogonal modes:

$$\mathbf{E}(\mathbf{r},t) = \sum_n a_n(t)\, \boldsymbol{e}_n(\mathbf{r}) \sin(\omega_n t + \phi_n(t))$$

$$= \sum_n \left(\alpha_n(t)\, \mathbf{e}_n(\mathbf{r})\, e^{i\omega_n t} + \alpha_n^*(t)\, \mathbf{e}_n^*(\mathbf{r})\, e^{-i\omega_n t} \right)$$

$$= \sum_n \left(A_n(t)\, \mathbf{e}_n(\mathbf{r}) + A_n^*(t)\, \mathbf{e}_n^*(\mathbf{r}) \right)$$

with complex amplitude:

$$A_n(t) = \alpha_n(t) e^{i\omega_n t} = \frac{a_n(t)}{2} e^{i(\omega_n t + \phi_n(t))}$$

and field form factors:

$$\mathbf{e}_n(\mathbf{r}) = \frac{\boldsymbol{e}_n(\mathbf{r})}{i}$$

that are solutions of the Helmoltz equations:

$$\nabla^2 \mathbf{e}_n + k_n^2 \mathbf{e}_n = 0$$

with the orthogonality conditions:

$$\int_v \mathbf{e}_k \cdot \mathbf{e}_n^* \, dv = \delta_{kn}$$

and the normalization relations:

$$|A_n(t)| = \sqrt{\frac{U_n(t)}{2\varepsilon}} \qquad |\mathbf{e}_n| = \sqrt{\frac{\varepsilon}{2U_{n.o}^{code}}} \mathbf{E}_{n.o}^{code}$$

where $\mathbf{E}_{n,o}^{code}$ are the electric field and $U_{n,o}^{code}$ the corresponding stored energy, as computed by the standard field codes (SUPERFISH, URMEL, etc.).

Considering only the longitudinal component on the cavity axis $e_n(z)=\mathbf{e}_n(r=0,z)$ the wave equation for the electric field complex amplitude in the cavity is:

$$\frac{d^2 A_n}{dt^2} + \omega_n^2 A_n = -\frac{1}{\varepsilon} \frac{d}{dt} \left[\int_V J \cdot e_n^*(z) \, dv \right]$$

As a driving current densities we consider the superposition of three terms $J = J_c + J_g + J_b$. The first term J_c is a dissipation current density on a point like dielectric on the cavity axis at z_c , representing the flow of energy out of the main coupler and the inter-mode energy exchange on the coupler position. We neglect the dissipation due to wall losses. The term J_g is a feeding sinusoidal current density , representing the power supply. The third term J_b represent the beam current density.

The dissipation term. - We consider an "ideal but lossy" cavity [11], i. e. a cavity with perfectly conducting walls but filled with a dielectric with finite conductivity σ. We assume the loss term mainly due to dissipation on the coupler port considering it as a point like dielectric on the cavity axis at the coupler position z_c.

From Ohm 's law we obtain:

$$J_c = \sigma\delta(z\text{-}z_c)E(z) = \sigma\delta(z\text{-}z_c)\sum_k A_k(t)e_k(z)$$

the integral becomes:

$$\frac{d}{dt}\left[\int_V J_c \cdot e_n^* dv\right] = \sigma\sum_k \frac{d}{dt}\left[A_k \int_V e_k \cdot e_n^* \, \delta(z\text{-}z_c)\, dv\right] = \sigma\sum_k \left[\frac{d}{dt}A_k\, e_k(z_c)\right] e_n^*(z_c)$$

and substituting in the wave equation:

$$\frac{d^2A_n}{dt^2} + \omega_n^2 A_n = -\frac{\sigma}{\varepsilon}\sum_k \left[\frac{d}{dt}A_k\, e_k(z_c)\right] e_n^*(z_c)$$

Setting now:

$$\frac{\omega_n}{Q_n} = \frac{\sigma}{\varepsilon}$$

we obtain:

$$\frac{d^2A_n}{dt^2} + \frac{\omega_n}{Q_n}\sum_k \left[e_k(z_c)\,\frac{dA_k}{dt}\right] e_n^*(z_c) + \omega_n^2 A_n = 0$$

where the term between brackets accounts for losses of mode n through the coupler and towards the others modes. We obtain therefore a system of N coupled equations [2].

The power supply term. - Considering now a driving term due to a generator represented by a sinusoidal current density on the coupler position z_g :

$$J_g = J_g \sin(\omega_1 t + \psi_g)\ \delta(z\text{-}z_g) = (J_g(t) + J_g^*(t))\ \delta(z\text{-}z_g)$$

where:

$$J_g(t) = \frac{J_g}{2i} e^{i(\omega_1 t + \psi_g)}$$

Setting:

$$E_1(z_g) = A_{g1} e_1(z_g)$$

and evaluating:

$$\int_V |J_g \delta(z\text{-}z_g) e_1^*(z)|dv = |J_g e_1(z_g)| = \left|\frac{J_g E_1(z_g)}{A_{g1}}\right| = \frac{\hat{P}_{g1}}{2|A_{g1}|}$$

$$= \frac{<P_{g1}>}{|A_{g1}|} = \frac{\omega_1 U_1}{|A_{g1}|Q_1} = \frac{\omega_1 2\varepsilon |A_{g1}|^2}{|A_{g1}|Q_1} = \frac{2\varepsilon\omega_1}{Q_1}|A_{g1}|$$

we can define the amplitude of the constant driving term as:

$$|J_g| = \frac{J_g}{2} = \frac{2\varepsilon\omega_1\ |A_{g1}|}{Q_1\ |e_1(z_g)|}$$

The driving integral becomes:

$$\frac{d}{dt}\left[\int_V J_g \bullet e_n^* dv\right] = \omega_1\left[\int_V J_g(t)\delta(z-z_g)e_n^*(z)\, dv\right] = \omega_1 J_g(t)e_n^*(z_g)$$

and setting:

$$K_g = \frac{2\omega_1^2 |A_{g1}|}{iQ_1 |e_1(z_g)|}$$

the wave equation becomes:

$$\frac{d^2 A_n}{dt^2} + \frac{\omega_n}{Q_n}\sum_k\left[e_k(z_c)\frac{d}{dt}A_k\right]e_n^*(z_c) + \omega_n^2 A_n = -K_g e_n^*(z_g)\, e^{i(\omega_1 t + \psi_g)}$$

The beam term. - The basic assumption in the description of beam dynamics consists in representing each bunch as a uniform charged cylinder, whose length L and radius R can vary under a self-similar evolution, i.e. keeping anyway uniform the charge distribution inside the bunch. The present choice of a uniform distribution is dictated just by sake of simplicity in the calculation of space charge and HOM contributions to the beam dynamics.

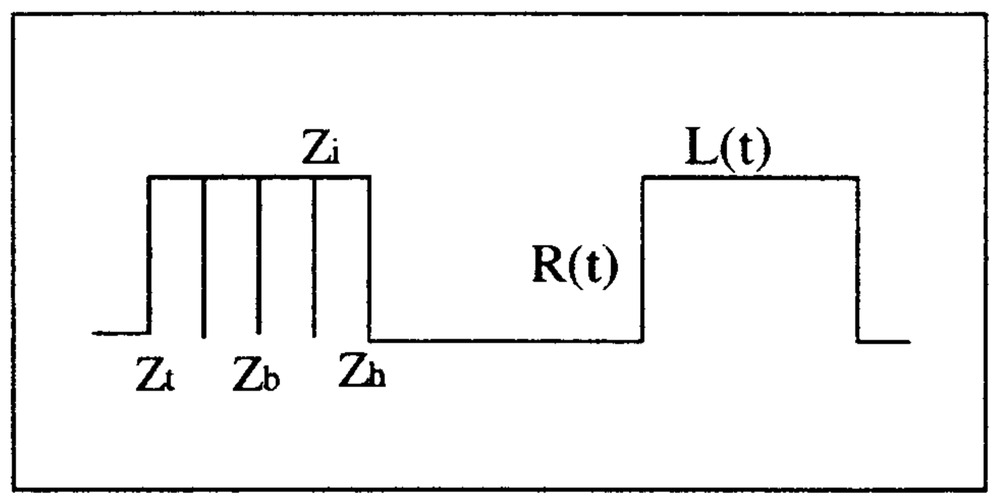

Figure C-1: Bunch representation in N-slices

The linear beam current density term J_b can be written for each bunch as follows:

$$J_b = \frac{q\beta_b c}{L}\left(\eta(z-z_t) - \eta(z-z_h)\right)$$

where η is a step function and the indexes b,h,t refer to bunch barycenter, head and tail position respectively.

The interaction term becomes:

$$\int_v \left(\frac{dJ_b}{dt} \bullet e_n\right) dv = \frac{d}{dt}\left[\frac{q\beta_b c}{L}\int_0^{L_{cav}} \left(\eta(z-z_t(t)) - \eta(z-z_h(t))\right) e_n^*(z)dz\right]$$

$$= \frac{d}{dt}\left[\frac{q\beta_b c}{L}\int_{z_t(t)}^{z_h(t)} e_n^*(z)dz\right]$$

$$= \frac{q\beta_b c}{L}\left(e_n^*(z_h)\frac{dz_h}{dt} - e_n^*(z_t)\frac{dz_t}{dt}\right) + qc\left(\frac{1}{L}\frac{d\beta_b}{dt} - \frac{\beta_b}{L^2}\frac{dL}{dt}\right)\int_{z_t(t)}^{z_h(t)} e_n^*(z)dz$$

$$= \frac{q\beta_b^2 c}{L}\left(e_n^*(z_h) - e_n^*(z_t)\right) + \frac{qc}{2}\left(e_n^*(z_h) + e_n^*(z_t)\right)\frac{d\beta_b}{dt}$$

where we made the approximation:

$$\int_{z_t(t)}^{z_h(t)} e_n^*(z)dz \approx \left[\frac{e_n^*(z_h)+e_n^*(z_t)}{2}\right] L$$

and we used the following identities:

$$\frac{dz_h}{dt} = \beta_b + \frac{1}{2}\frac{dL}{dt} \qquad \frac{dz_t}{dt} = \beta_b - \frac{1}{2}\frac{dL}{dt}$$

The full wave equation becomes now:

$$\frac{d^2A_n}{dt^2} + \frac{\omega_n}{Q_n}\sum_k\left[e_k(z_t)\frac{d}{dt}A_k\right]e_n^*(z_t) + \omega_n^2 A_n = -K_g e_n^*(z_g)\, e^{i(\omega_1 t + \psi_g)} +$$

$$-\frac{1}{\varepsilon}\left[\frac{q\beta_b^2 c}{L}\left(e_n^*(z_h) - e_n^*(z_t)\right) + \frac{qc}{2}\left(e_n^*(z_h) + e_n^*(z_t)\right)\frac{d\beta_b}{dt}\right]$$

The Slowly Varying Envelope Approximation. - Substituting in the previous equation $A_n(t) = \alpha_n(t)e^{i\omega_n t}$ and applying the SVEA approximation hypotheses:

$$\frac{d\alpha_n}{dt} << \omega_n\alpha_n \qquad \frac{d^2\alpha_n}{dt^2} << \omega_n^2\alpha_n$$

we can neglect the second order derivative and we obtain the first order equation for each mode:

$$\frac{d\alpha_n}{dt} + \frac{1}{2Q_n}\left(1+\frac{i}{2Q'_n}\right)\sum_k \omega_k \alpha_k e_k(z_j) e^{i\Omega_{k,n}t} =$$

$$= \frac{i}{2\omega_n}\left(1+\frac{i}{2Q'_n}\right)\left\{ K_g e_n^*(z_g)\, e^{i(\Omega_{1,n}t + \psi_g)} + \right.$$

$$\left. + \frac{1}{\varepsilon}\left[\frac{q\beta_b^2 c}{L}\left(e_n^*(z_h) - e_n^*(z_j)\right) + \frac{qc}{2}\left(e_n^*(z_h) + e_n^*(z_j)\right)\frac{d\beta_b}{dt}\right] e^{-i\omega_n t}\right\}$$

where we defined the detuning shift $\Omega_{k,n} = (\omega_k - \omega_n)$, $\Omega_{1,n} = (\omega_1 - \omega_n)$ and $Q'_n = \frac{Q_n}{|e_n|^2}$.

THE BEAM EQUATIONS

The equations for the longitudinal motion of the bunch barycenter are:

$$\frac{dz_b}{dt} = \beta_b c \qquad \frac{d\beta_b}{dt} = \frac{e}{m_o c \gamma_b^3} E_z(z_b,t)$$

The bunch lengthening is simply given by the head-tail velocity difference:

$$\frac{dL}{dt} = c\left(\beta_h - \beta_j\right)$$

The energy spread inside the bunch is derived by specifying the energy associated with N slices each one located at a different position z_i and adding to the first order component coming from fundamental and HOM modes, the space charge effects:

$$\frac{d\gamma_i}{dt} = \frac{e}{m_o c}\beta_i\left[E_z(z_i,t) + E_z^{sc}(\tilde{z},t)\right]$$

where i=1,N and N is the number of slices.

The longitudinal and radial space charge fields at a distance $\tilde{z} = z_i - z_t$ from the bunch tail, see figure C-1, are given by [12]:

$$E_z^{sc}(\tilde{z}) = \frac{q}{2\pi\varepsilon_o \gamma_b R^2 L}\left(\sqrt{\gamma_b^2(L-\tilde{z})^2 + R^2} + \gamma_b(2\tilde{z}-L) - \sqrt{(\gamma_b\tilde{z})^2 + R^2}\right)$$

$$E_r^{sc}(\tilde{z}) = \left(\frac{\rho}{\varepsilon_o} - \frac{dE_z}{d\tilde{z}}\right)\frac{R}{2} = \frac{\gamma_b q}{4\pi\varepsilon_o RL}\left\{\frac{\tilde{z}}{\sqrt{(\gamma_b\tilde{z})^2 + R^2}} + \frac{(L-\tilde{z})}{\sqrt{\gamma_b^2(L-\tilde{z})^2 + R^2}}\right\}$$

where $\rho = \frac{q}{\pi R^2 L}$ is the charge density.

The evolution of the bunch radius R is described according to the envelope equation under a quasi-laminar flow approximation [13], including RF-focusing (first term), space charge effects (second), thermal emittance (third), damping due to acceleration (fourth) and solenoidal lens (fifth), transformed into the time-domain:

$$\frac{d^2 R_i}{dt^2} = -\frac{eR_i}{2\gamma_b m_o c}\left[c\frac{\partial E_z(z,t)}{\partial z} + \beta_b \frac{\partial E_z(z,t)}{\partial t}\right] + \frac{qE_r(R_i,\tilde{z})}{m_o \gamma_b^3}$$

$$+ \frac{(\varepsilon_{n,o} c)^2}{\gamma_b^2 R_i^3} - \beta_b \gamma_b^2 \frac{d\beta_b}{dt}\frac{dR_i}{dt} - \left[\frac{eB_z(z)}{2m_o\gamma_b}\right]^2 R_i$$

where ε_n is the rms normalized beam emittance and the RF focusing force $F^{rf}=e[E_r(r,z,t)-\beta c B_\theta(r,z,t)]$ has been expressed through the linear expansion off-axis of the $E_Z(o,z,t)$ field.

In order to evaluate the degradation of the rms emittance produced by longitudinal correlation in space charge and RF forces, we use the following expression for the correlated emittance:

$$\varepsilon_c = \frac{\langle \beta\gamma \rangle}{N}\sqrt{\sum_i R_i^2 \sum_i R'^2_i - \left(\sum_i R_i R'_i\right)^2}$$

where N is the number of slices, R_i is the i-th slice radius, R'_i its divergence and $\varepsilon_{n,o}$ the thermal emittance. The total rms emittance will be given by quadratic summation of the thermal emittance and correlated emittance:

$$\varepsilon_n = \sqrt{\varepsilon_{n,o}^2 + \varepsilon_c^2}$$